Spatiotemporal dynamics of nektonic biodiversity and vegetation shifts during the Smithian–Spathian transition: conodont and palynomorph insights from Svalbard

Leu, Marc ; Schneebeli Hermann, Elke ; Hammer, Øyvind ; Lindemann, Franz Josef ; Bucher, Hugo

DOI: https://doi.org/10.18261/let.57.2.3

Lethaia
AN INTERNATIONAL JOURNAL OF PALAEONTOLOGY AND STRATIGRAPHY

Spatiotemporal dynamics of nektonic biodiversity and vegetation shifts during the Smithian–Spathian transition: conodont and palynomorph insights from Svalbard

MARC LEU, ELKE SCHNEEBELI-HERMANN, ØYVIND HAMMER, FRANZ-JOSEF LINDEMANN, HUGO BUCHER

LETHAIA

The Smithian–Spathian transition (~249.2 Ma) is marked by profound environmental changes, carbon cycle perturbations, and the stepwise loss of nektonic biodiversity (ammonoids and conodonts). While biotic and abiotic changes have been intensely studied for the palaeosubtropics and palaeotropics, the global spatio-temporal pattern, including mid- to higher latitudes, remains unresolved. In this study, we present conodont and palynomorph data from the Lower Triassic Vikinghøgda Formation in the Stensiöfjellet section, Svalbard. Conodont samples from this sequence generally yielded relatively few specimens with one exception in the basal Vendomdalen Member, which proved exceptionally abundant and diverse. Most conodont samples of the Lusitaniadalen Member are typically dominated by middle to late Smithian segminiplanate forms, such as *Scythogondolella* spp. This exceptional horizon in the basal Vendomdalen Member, associated with the cosmopolitan ammonoid *Bajarunia*, indicates an earliest Spathian age. This sample presents the first-ever recorded conodont fauna from the earliest Spathian in the Boreal realm and associates segminiplanate with numerous segminate forms. The presence of an abundant and diverse segminate conodont fauna in northern mid-latitudes during the Early Triassic suggests that temperature was not the main regulator for their distribution, as opposed to segminiplanate forms, which were apparently more restricted to colder waters. Palynomorphs are poorly preserved but allow the discrimination of three assemblages. Association 1 is lycophyte spore dominated, and associations 2 and 3 are both dominated by bisaccate pollen. The change from lycophyte-dominated to a gymnosperm-dominated vegetation occurs just above the *Wasatchites* beds. A comparison with the records from the southern palaeosubtropics indicates that the vegetation shift was synchronous and coincided with the onset of a cooling episode, commencing in the latest Smithian. □ *Intra-Triassic extinction, palaeoclimate, palaeoenvironment, conodonts, palynomorphs, Svalbard.*

Marc Leu ✉ [marc.leu@pim.uzh.ch], Elke Schneebeli-Hermann [ehermann@pim.uzh.ch] and Hugo Bucher [bucherhugo9@pim.uzh.ch] Department of Palaeontology, University of Zurich, Karl Schmid-Strasse 4, 8006 Zurich, Switzerland; Øyvind Hammer [oyvind.hammer@nhm.uio.no] and Franz-Josef Lindemann [f.j.lindemann@nhm.uio.no], Natural History Museum, University of Oslo, Pb. 1172 Blindern, 0318 Oslo, Norway; *manuscript received on 04/08/2023; manuscript accepted on 28/02/2024; manuscript published on 20/06/2024 in* Lethaia 57(2).

Lower Triassic palaeontological records are characterized by complex patterns of slow recovery of benthic organisms and explosive radiations and subsequent extinctions in nektonic clades (e.g. Orchard 2007; Brayard *et al.* 2009; Hautmann 2014; Friesenbichler *et al.* 2021). The most remarkable of these extinction events occurred close to the Smithian–Spathian boundary; ammonoids and conodonts are the two nektonic groups that suffered most from the extinction event in the late Smithian. Prionitidae and Flemingitidae were two ammonoid families that went extinct (Brayard *et al.* 2006, and references therein). The conodont subfamilies Mullerinae and Scythogondolellinae were also victims of the late Smithian extinction (Orchard 2007). Additionally, marine predatory vertebrate faunas underwent a major restructuring. The dominant apex predators in the Smithian were the temnospondyl amphibians and the fishes, whereas in the Spathian marine reptiles were dominant (Scheyer *et al.* 2014).

On land, a change in vegetation composition is observed across different biomes. Palynological data from northern mid-latitude successions of Greenland and the Barents Sea (Galfetti *et al.* 2007c; Lindström *et al.* 2019) and from the North Indian Margin in the southern subtropics document a shift from a lycophyte-dominated vegetation in the Smithian to a gymnosperm-dominated vegetation in the Spathian (Hermann *et al.* 2011; Schneebeli-Hermann *et al.* 2012). Biomarker data from South China indicate

https://doi.org/10.18261/let.57.2.3

a similar change in the tropics (Saito *et al.* 2013). In Pakistan, where a detailed biostratigraphical age control is given, this shift in plant associations is dated to occur just above the late Smithian *Wasatchites* beds (Hermann *et al.* 2012).

The changes in the marine realm and the shift in continental vegetation are associated with perturbations in the carbon cycle, which are reflected in a negative and positive anomaly in $\delta^{13}C$ records from the middle Smithian to the early Spathian (e.g. Galfetti *et al.* 2007a, Zhang *et al.* 2019). Climatic conditions were unstable, too. Conodont apatite oxygen isotopes from the southern subtropics of Pakistan (Goudemand *et al.* 2019) indicate that the warm climate of the middle Smithian culminated in the early late Smithian, followed by an abrupt cooling in the late Smithian and earliest Spathian.

Precise biostratigraphical dating in combination with U-Pb calibration is well established for low latitudes (e.g. Galfetti *et al.* 2007a; Chen *et al.* 2019; Zhang *et al.* 2019; Widmann *et al.* 2020; Leu *et al.* 2022, 2023), whereas for mid-latitudes, a detailed timeline of events is still missing. To decipher potential triggers for the Smithian-Spathian changes, it is essential to know whether biotic and abiotic changes around the Smithian-Spathian boundary in low and mid-latitudes are synchronous or not. Therefore, we investigate the timing of changes in vegetation and conodont population at a northern mid-latitude site.

Geological, stratigraphical, and palaeogeographical setting

On the Svalbard archipelago, Lower Triassic sediments were deposited in a marine epicontinental basin, lying between 45 and 60°N (Mørk *et al.* 1982). Shallow marine and coastal deposits in Spitsbergen are represented by the Vardebukta (Griesbachian to Dienerian) and the Tvillingodden (Smithian–Spathian) formations. The distal equivalent in central and eastern Spitsbergen, as well as on Barentsøya and Edgeøya, is the Lower Triassic Vikinghøgda Formation (Fig. 1). It comprises shales, siltstones, sandstones, and horizons with calcareous nodules. The Vikinghøgda Formation is subdivided into the Deltadalen (Griesbachian to Dienerian), the Lusitaniadalen (~Smithian), and the Vendomdalen (~Spathian) members. Sediment transport occurred from the west (Mørk *et al.* 1982, 1999). The upper fossiliferous part of the Lusitaniadalen Member corresponds to the so-called 'fish niveau' (Wiman 1910, Stensiö 1921). The lithostratigraphical base of the Vendomdalen Member is defined by the top of a yellow-weathering cemented siltstone (Mørk *et al.* 1999). Generally, this boundary corresponds to a shift from grey shales of the Lusitaniadalen Member to dark grey paper shales of the Vendomdalen Member. The rather abrupt positive shift in $\delta^{13}C_{org}$ in the Wallenbergfjellet section (~5 km S of Stensiöfjellet) suggests a hiatus in the latest Smithian (Hammer *et al.* 2019).

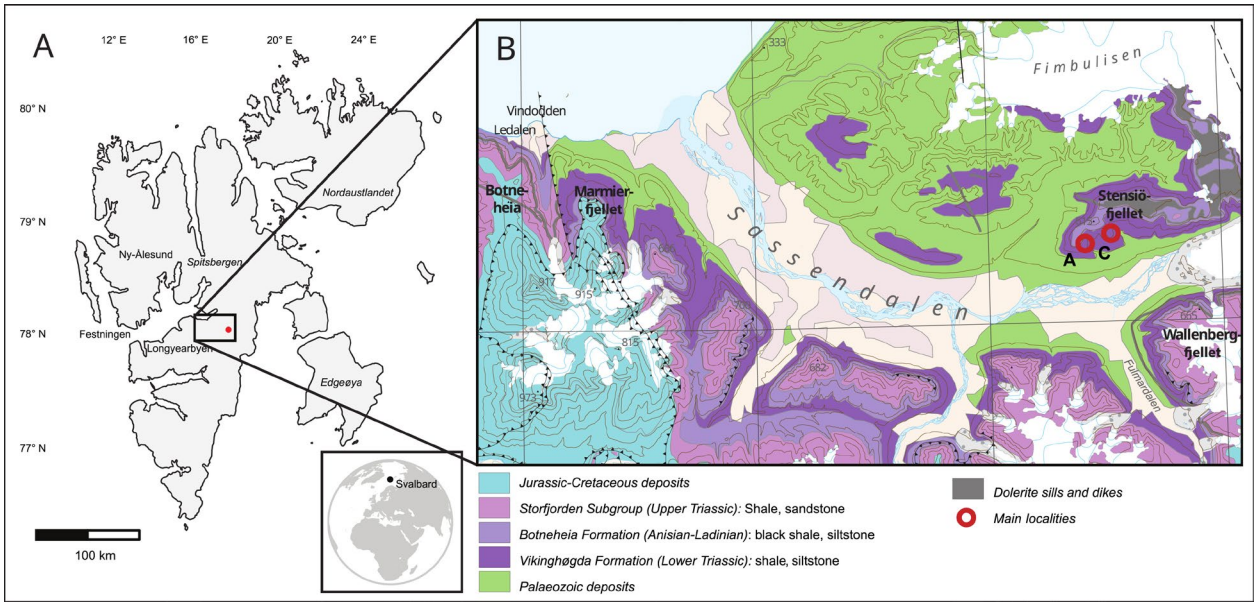

Fig. 1. Map of Svalbard and the locations of the study sites on the main island Spitsbergen. A, overview map of Svalbard. B, geological map of Sassendalen area, redrawn after https://geokart.npolar.no/geologi/GeoSvalbard. The two main studied localities are indicated with red circles, STA with A and STC with C.

Ammonoid assemblages of the middle Smithian *Euflemingites romunduri* Zone (Lusitaniadalen Member) are dominated by the genus *Arctoceras* (Hansen *et al*. 2021). This zone is directly overlain by the early late Smithian *Wasatchites tardus* Zone (Weitschat & Lehmann 1978; Piazza *et al*. 2017). This zone is a correlative of the low-latitude *Anasibirites multiformis* Zone and the only late Smithian ammonoid zone in the Boreal realm. On the North Indian Margin and in the Western USA Basin, the *A. multiformis* Zone is followed by the *Glyptophiceras sinatum* beds (Unitary Association SM-13, Brühwiler *et al*. 2010). The Smithian–Spathian boundary is located in an interval of separation between the *G. sinatum* beds and the tirolitid n. gen. A beds (Galfetti *et al*. 2007c; Widmann *et al*. 2020). However, the ammonoid-based position of the Smithian–Spathian boundary in low latitudes is not readily transferable to the northern mid-latitude sections because *Glyptophiceras sinatum* is missing there and tirolitid diversification is restricted to low latitudes (Fig. 2 and Hammer *et al*. 2019). At Stensiöfjellet, the cosmopolitan ammonoid *Bajarunia* sp. indicates an early Spathian age for the basal Vendomdalen Member (Hammer *et al*. 2019). In the type section of the Vikinghøgda Formation, carbonate nodules close to the top of the Vendomdalen Member contain the late Spathian ammonoid fauna with *Keyserlingites subrobustus*, *Svalbardiceras spitzbergense*, and *Popovites occidentalis* (Weitschat & Dagys 1989; Mørk *et al*. 1999). At Wallenbergfjellet and Stensiöfjellet late Spathian ammonoids were documented down into the middle part of the Vendomdalen Member; the lower part of the member includes horizons of condensation and/or non-deposition (Hansen *et al*. 2024).

The Smithian-Spathian boundary, as it pertains to conodont biostratigraphy, is situated between two Unitary Association Zones (UAZ3 and UAZ4 in Oman, UAZ7 and UAZ8 in South China), according to Leu *et al*. (2022, 2023). Like ammonoid zones, the latest Smithian conodont zones are also absent in the Boreal realm compared to lower latitudes. Within the Lusitaniadalen Member, the conodont species *Scythogondolella milleri*, *Sc. mosheri*, *Borinella* aff. *buurensis*, and *Neospathodus waageni* coexist with the late Smithian ammonoid *Wasatchites tardus* in its uppermost segment (Weitschat & Lehmann 1978; Nakrem *et al*. 2008). The *W. tardus* zone can be correlated with the conodont UAZ6 in China and UAZ1 in Oman (Leu *et al*. 2022, 2023), indicating that only the first of the late Smithian conodont zones is present in the Lusitanidalen Member.

Before this study, the lower part of the Vendomdalen Member was considered devoid of conodonts. *Columbitella*? *paragondolellaeformis* and *Neogondolella* ex. gr. *regalis* appear only in the upper part of the Vendomdalen Member in association with the ammonoids *Keyserlingites subrobustus* and *Svalbardiceras spitzbergense* (Nakrem *et al*. 2008).

Smithian and Spathian palynomorphs have earlier been studied from several successions on Spitsbergen,

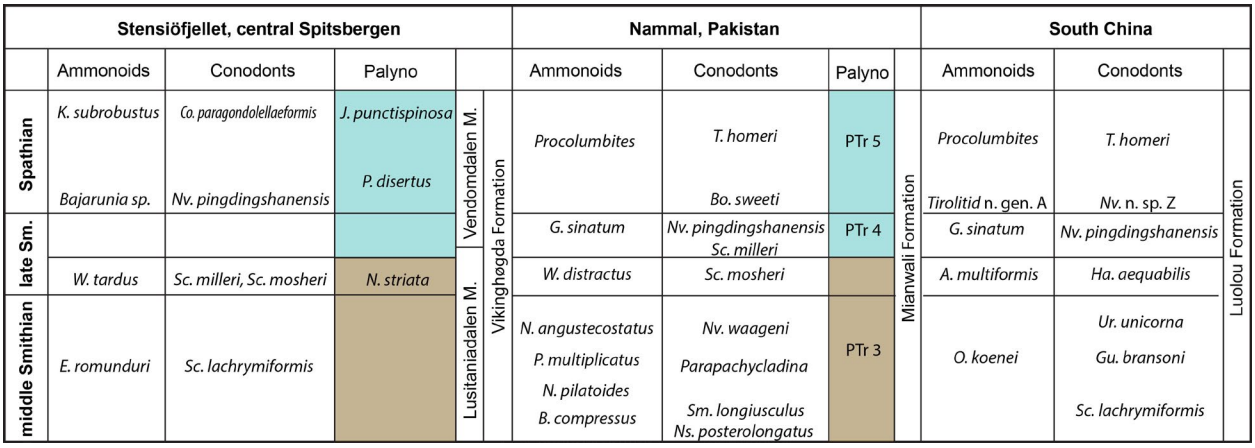

Fig. 2. Comparison of ammonoid, conodont and palynozones from Svalbard (after Weitschat & Dagys 1989; Hammer *et al*. 2019; Nakrem *et al*. 2008 and Vigran *et al*. 2014); Pakistan (Brühwiler *et al*. 2010, Romano *et al*. 2013 and Hermann *et al*. 2012) and South China (Galfetti *et al*. 2007b and Leu *et al*. 2022). Please note that only key representative conodont species are indicated. Abbreviations. late Sm. = late Smithian, *K. subrobustus = Keyserlingites subrobustus, W. tardus = Wasatchites tardus, E. romunduri = Euflemingites romunduri, G. sinatum = Glyptophiceras sinatum, W. distractus = Wasatchites distractus, N. angustecostatus = Nyalamites angustecostatus, P. mutiplicatus = Pseudoceltites multiplicatus, N. pilatoides = Nammalites pilatoides, B. compressus = Brayardites compressus, A. multiformis = Anasibirites multiformis, O. koenei = Owenites koenei, Co. = Columbitella, Nv. = Novispathodus, Sc. = Scythogondolella, T. = Triassospathodus, Bo. = Borinella, Sm. = Smithodus, Ns. = Neospathodus, Ha. = Hadrodontina, Ur. = Urdyella, Gu. Guangxidella, J. punctispinosa = Jerseyiaspora punctispinosa, P. disertus = Pechorosporites disertus.* Brown colour indicates spore dominated palynomorph assemblages, blue colour indicates pollen-dominated palynomorph assemblages.

Barentsøya, and Edgeøya, including a few samples from the Stensiöfjellet section (Vigran *et al.* 2014). Sediments of the Lusitaniadalen Member include palynomorphs of the *Naumovaspora striata* Composite Assemblage Zone. These are characterized by a dominance of spores, especially in the upper part of the zone. Common spores in this zone are *Densoisporites playfordii* and *Punctatisporites fungosus*. Fungal remains occur regularly and more abundantly in the upper part of the zone. These assemblages co-occur with *Euflemingites romunduri* Tozer, 1961 and are thus of Smithian age. Assemblages of the lower part of the Vendomdalen Member are assignable to the *Pechorosporites disertus* Composite Assemblage Zone. These show a relative high abundance of bisaccate pollen grains. *Pechorosporites disertus* is a typical spore taxon in this zone, and together with the first appearance of *Cordaitina gunyalensis*, the common occurrence of this spore was used to define the base of this zone (Vigran *et al.* 2014). Age assignment is based on correlation with the palynozone 'Svalis-3' of Vigran *et al.* (1998), and Assemblage M of Hochuli *et al.* (1989), from the Svalis Dome. The assemblages of the Svalis Dome area have been correlated with Russian palynological data, which indicates an early Spathian age (Vigran *et al.* 1998, 2014). The uppermost Lower Triassic palynozone is the *Jerseyiaspora punctispinosa* Composite Assemblage Zone, which is characterized by abundant taeniate bisaccate pollen (*Lunatisporites* spp., *Striatoabieites* spp.). Cavate spores are relatively diverse. *Cyclotriletes pustulatus* and *Jerseyiaspora punctispinosa* are among the spore taxa that have their first appearance in this zone. Prasinophytes (*Tasmanites* spp.) are dominant in many successions. The assemblages were documented from intervals straddling the *Keyserlingites subrobustus* Zone, which dates the *Jerseyiaspora punctispinosa* Composite Assemblage Zone as late Spathian (Vigran *et al.* 2014). To date, only five samples have been studied from the entire interval of the Lusitaniadalen and Vendomdalen members at Stensiöfjellet, whereas higher palynological resolution is available for nearby successions such as Milne Edwardsfjellet and Vikinghøgda. The lowest sample from the middle of the Lusitaniadalen Member has been assigned to the *Naumovaspora striata* Composite Assemblage Zone; the second sample, located close to the Lusitaniadalen–Vendomdalen boundary, has been tentatively assigned to the *Pechorosporites disertus* Composite Assemblage Zone; and the uppermost three samples from the upper part of the Vendomdalen Member to the *Jerseyiaspora punctispinosa* Composite Assemblage Zone (Vigran *et al.* 2014).

Lower Triassic carbon cycle perturbations are reflected in repeated positive and negative anomalies (e.g. Galfetti *et al.* 2007a). Middle Smithian carbon isotope records ($\delta^{13}C$) are marked by a negative shift followed by a positive shift in the late Smithian to early Spathian. Various positions of this positive shift have been debated as markers for the Smithian–Spathian boundary. While at Festningen (West Spitspergen) the onset of the positive shift has been favoured (Grasby *et al.* 2016), in South China, ammonoids suggest that the boundary is closer to the maximum in $\delta^{13}C$ values (Galfetti *et al.* 2007a), which is substantiated by the positive peak lying in the basal Vendomdalen Member (Galfetti *et al.* 2007a; Hammer *et al.* 2019). A comparison of ammonoid and/or conodont calibrated $\delta^{13}C$ records indicates that the Smithian–Spathian boundary is allocated within the positive flank of the $\delta^{13}C$ excursion (Zhang *et al.* 2019). The abrupt positive shift documented in the Wallenbergfjellet succession indicates a sedimentary hiatus (Hammer *et al.* 2019). CA-ID-TIMS U-Pb dates refined the age of the Smithian–Spathian boundary to a period between 249.29 ± 0.06 and 249.11 ± 0.09 Ma (Widmann *et al.* 2020).

Material and methods

Two main sections were logged, Stensiöfjellet A and Stensiöfjellet C sections, ca. 1.2 km apart and samples were taken from them. For conodonts, we collected 17 samples, each weighing approximately 10kg, from section Stensiöfjellet C. Of the 17 samples, 11 were taken from the Lusitaniadalen Member and 6 from the Vendomdalen Member, with varying spacing between samples ranging from 1 m to 60 m. The samples were dissolved using a ~10% buffered acetic acid solution following the procedure described by Jeppsson *et al.* (1999). The residues were concentrated by using sodium polytungstate (Jeppsson & Anehus 1999) as a heavy liquid for separation. They were then sieved using a 0.075-mm mesh, and the heavy fraction was handpicked under a binocular microscope. The selected conodont elements were illustrated using a scattered electron microscope (SEM) (JEOL JSM-6010) without the use of a sputter coater, and a digital microscope (Keyence VHX 6000).

For palynological analysis, samples (n = 61 Stensiöfjellet A, Fig. 1) were cleaned, crushed, and weighed (15 g on average) and subsequently treated with concentrated hydrochloric and hydrofluoric acid as described by Traverse (2007). The residues were sieved over a 11-µm mesh screen. Samples were additionally treated with concentrated nitric acid and 30 s of ultrasonic vibration. Residues were sieved again over an 11-µm mesh screen. Slides are stored in the repository of the Palaeontological Institute and

Museum, University of Zurich, under the accession numbers PIMUZ A/VI 163 to PIMUZ A/VI 166.

Results

Conodonts

Conodonts recovered from the Stensiöfjellet section C are relatively well preserved with a Conodont Alteration Index (CAI) of 1–1.5, resulting in the maximum temperature reached by the surrounding sedimentary rock of <100°C. However, conodont elements are considered usually rare, here defined as samples with fewer than 10 P_1 elements (with the exception of sample STC4). Many specimens are broken, making it challenging to identify them at the species level (e.g. *Scythogondolella* sp. indet. from STC5 or *Magnigondolella* sp. indet. from STC6).

The Lusitanidalen Member is dominated by conodont faunas of the genus *Scythogondolella,* whereas the base of the Vendomdalen Member is rich and abundant in both segminate and segminiplanate forms. The upper part of the Vendomdalen Member is relatively poor in conodonts, only a very few elements could be retrieved. Five local maximal horizons (LMHs) were identified where only determinable specimens were considered.

Ammonoid zones (Fig. 3) were applied from our own findings (Hansen *et al.* 2021, Locatelli 2023) and modified after Nakrem *et al.* (2008), Dagys & Weitschat (1993), Mørk *et al.* (1999), and Hounslow *et al.* (2008). The middle Smithian *A. blomstrandi* group 1 Zone is based on the work of Hansen *et al.* (2021), which clearly observed stratigraphically distinct groups of this species.

In Siberia, *Sibirites elegans* occurs in the *Efimovae* subzone, which is the last subzone of the *Grambergia* Zone (Dagys 1999). New data from H. Bucher (pers. coll.) from the Northern Humboldt Range shows that both *Sibirites* and *Olenekites* are restricted to the middle Spathian *Prohungarites gustadti* beds (see also Guex *et al.* 2010, fig. 14).

Therefore, a middle Spathian age can be assumed for *Sibirites elegans* at Milne Edwardsfjellet (Hunslow *et al.* 2008). This species was first mentioned by Mørk *et al.* (1999) under the name *Parasibirites* cf. *elegans*. Comparable thickness of the Vendomdalen Member at Milne Edwardsfjellet and Stensiöfjellet allows the projection of stratigraphical positioning of *S. elegans* from the first into the second section across a distance of ca. 5km.

Furthermore, the condensed horizon of the *Grippia* bonebed (Hansen *et al.* 2018) correlates to the *Bajarunia euomphala* Zone or *Parasibirites grambergi* Zone, which makes it either early or early/middle Spathian in age. Based on the magnetic susceptibility curve from Milne Edwardsfjellet (Hounslow *et al.* 2008), we can also project the condensed horizon ca. 10m above the base of the Vendomdalen Member at Stensiöfjellet. Higher magnetic susceptibility rates often coincide with lower sedimentation rates i.e. condensed sections (e.g. Da Silva & Boulvain 2006 Blaha *et al.* 2008). Notably, a recent study by Nakrem & Orchard (2023) described conodonts from the *Grippia* bonebed, providing crucial insights into the age of this unit and confirming a late early Spathian age.

Conodont Local Maximal Horizons (LMH)

A Local Maximal Horizon (LMH) is a specific stratigraphical layer characterized by a unique association of species that cannot be subsumed under any larger set. These unique associations within an LMH are crucial as they serve as chronological markers, aiding in the distinction of different time intervals (Guex 1991).

For identifying biochronozones with the highest possible resolution, it is relevant to focus on samples where the set of occurring species is maximal, defined as LMHs, representing the initial step in creating Unitary Association zones (UAZs), in turn providing a foundation for biostratigraphical analysis and chronological delineation of geological time intervals (Guex 1991; Guex *et al.* 2016). However, for this study, we do not create UAZs as our analysis is confined to a single stratigraphical section.

LMH1.- Content: *Guangxidella bransoni* and *Scythogondolella lachrymiformis*. Sample: STC10. Age: middle Smithian.

This LMH is located within the ammonoid *E. romunduri* Zone (Fig. 3, ammonoid zones modified after Hansen *et al.* (2021), in which the *E. romunduri* Zone overlays the *A. blomstrandi* Group I Zone). The co-occurrence of *Gu. bransoni* with *Sc. lachrymiformis* (Fig. 4P) had already been observed from other Boreal regions within the *E. romunduri* Zone, such as the Canadian Arctic and British Columbia (Orchard 2008).

LMH2.- Content: *Scythogondolella lachrymiformis, Scythogondolella mosheri, Scythogondolella* ex gr. *milleri* and *Scythogondolella crenulata.* Sample: STC3. Age: middle/late Smithian.

LMH2 is dominated by species of the genus *Scythogondolella*. The LMH coincides with the upper end of the *E. romunduri* Zone. The co-occurrence of *Sc. lachrymiformis* (Fig. 5G) and *Sc. crenulata* (Fig. 5A) with *Sc. mosheri* (Figs 4Q, 5F) and *Sc.* ex gr. *milleri*

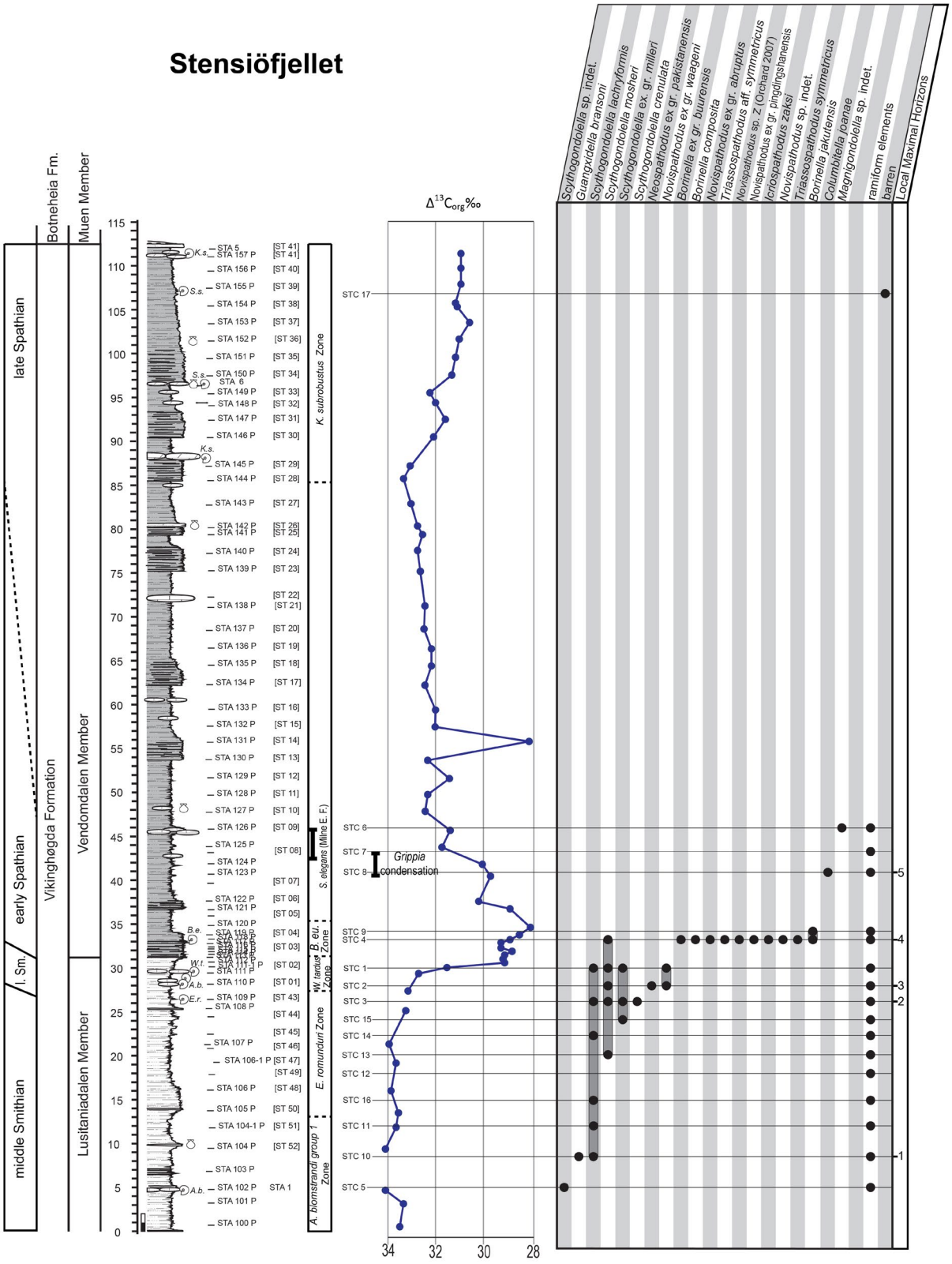

Fig. 3. Conodont, ammonoid and organic carbon isotopic stratigraphy at Stensiöfjellet, Spitsbergen. The local maximum horizons based on conodonts are indicated. The approximate position of the middle Spathian based on the intercalibrated occurrence of *Sibirites elegans* from Milne Edwardsfjellet is indicated (see Hounslow *et al.* 2008). Ammonoid findings are indicated with symbols. Ammonoid fauna modified after Hansen et al. 2018, 2020) Abbreviations: l. Sm.; late Smithian. *B. eu. & B.e.; Bajarunia euomphala. A. blomstrandi & A.b.; Anasibirites blomstrandi. E. romunduri & E.r.; Euflemingites romunduri. W. tardus & W.t.; Wasatchites tardus. K.s.; Keyserlingites subrobustus. S.s.; Svalbardiceras spitsbergense.*

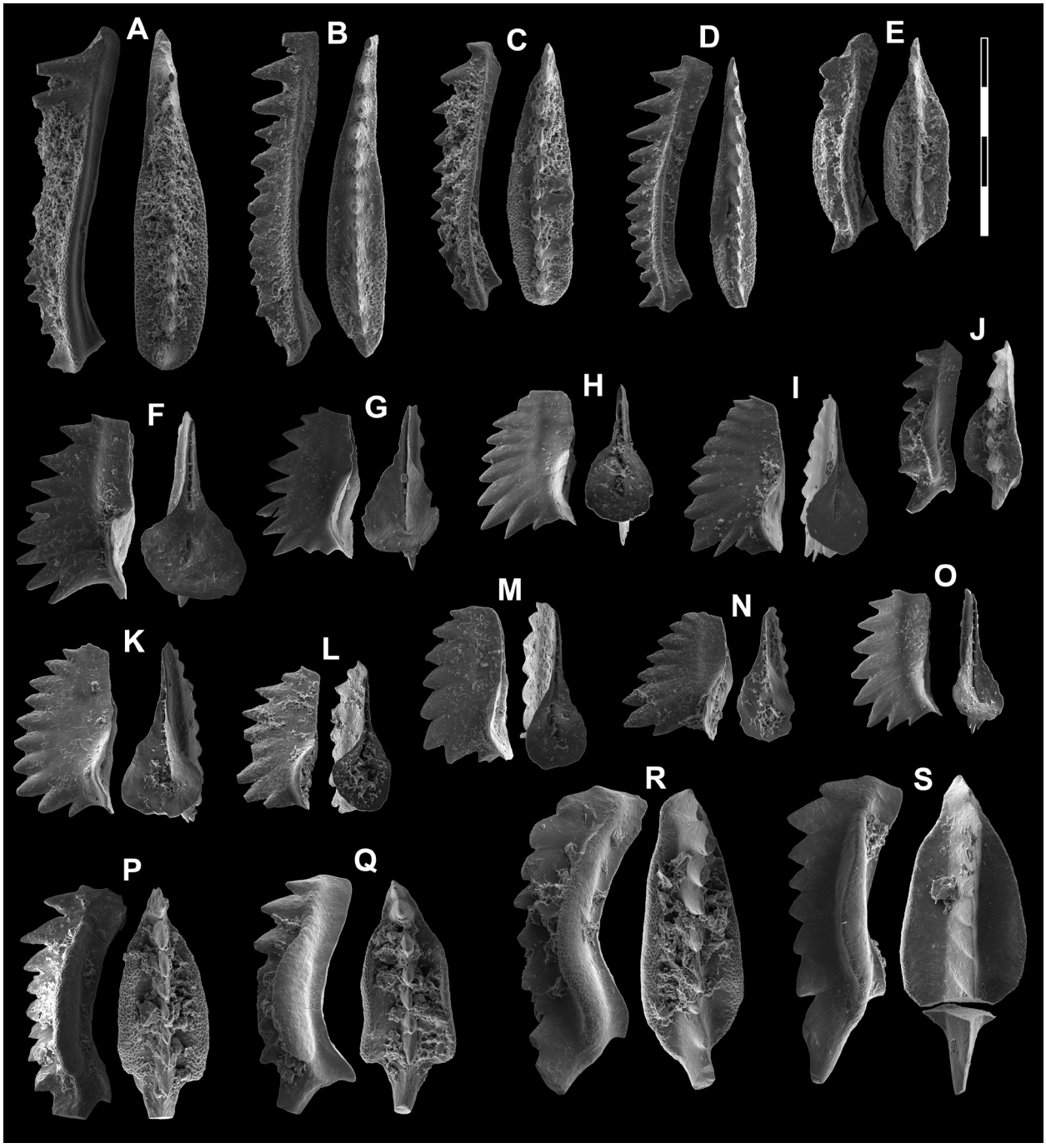

Fig. 4. SEM. The magnification is x80. Scale bar represents 400 μm. All specimens are P_1 elements if not otherwise specified. The orientation is standardized with the anterior side to the top, and the denticle tips to the left in 'lateral' views. Images were obtained with Scanning Electron Microscopy (SEM) (JEOL JSM-6010). A, *Borinella* ex gr. *buurensis* morphotype δ (Dagis 1984); STC4 (PIMUZ 40066). B, *Borinella jakutensis* Dagis 1984; STC4 (PIMUZ 40067). C, *Borinella* ex gr. *buurensis* morphotype α (Dagis 1984); STC4 (PIMUZ 40068). D, *Borinella composita*, Dagis 1984; STC4 (PIMUZ 40069). E, *Columbitella joanae* (Orchard 2009); STC8 (PIMUZ 40080). F, *Novispathodus* ex gr. *abruptus*? (Orchard 1995); STC4 (PIMUZ 40070). G, H, K, *Novispathodus* ex gr. *abruptus* (Orchard 1995); all STC4 (PIMUZ 40071, PIMUZ 40072, PIMUZ 40075). I, *Novispathodus* sp. Z (Leu & Goudemand 2022); STC4 (PIMUZ 40073). J, Q, *Scythogondolella mosheri* (Kozur & Mostler 1976); J, STC4 (PIMUZ 40074); Q, STC3 (PIMUZ 40045). L, *Icriospathodus zaksi* (Buryi 1979); STC4 (PIMUZ 40076). M, *Novispathodus* ex gr. *pingdingshanensis* (Zhao & Orchard 2005); STC4 (PIMUZ 40077). N, *Novispathodus* aff. sp. Z (Leu & Goudemand 2022); STC4 (PIMUZ 40078). O, *Triassospathodus* aff. *symmetricus* (Leu & Goudemand 2022); STC4 (PIMUZ 40079). P, *Scythogondolella lachrymiformis*? (Orchard 2008) STC10. R, *Scythogondolella lachrymiformis* (Orchard 2008); STC16 (PIMUZ 40088). S, *Scythogondolella mosheri*? (Kozur & Mostler 1976); STC14 (PIMUZ 40087).

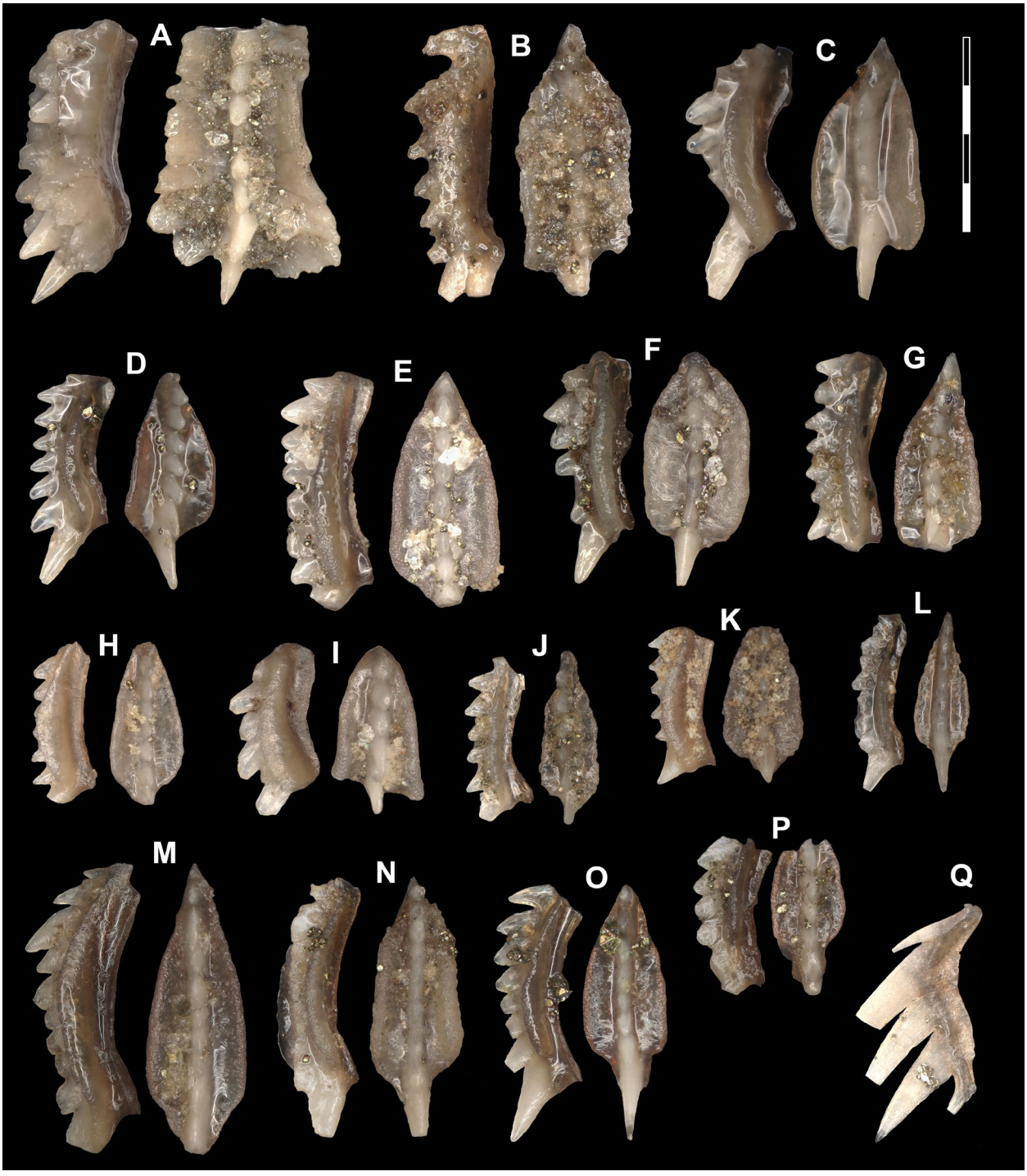

Fig. 5. digital microscope. The magnification is x80. Scale bar represents 400 μm. All specimens are P_1 elements if not otherwise specified. The orientation is standardized with the anterior side to the top, and the denticles tips to the left in 'lateral' views. Images were obtained with a Keyence VHX 6000 digital microscope. A, *Scythogondolella crenulata* (Mosher 1973); STC3 (PIMUZ 40040). B, J, *Scythogondolella* ex gr. *milleri* (Müller 1956); B, STC3 (PIMUZ 40041); J, STC1 (PIMUZ 40035). C, D, E, *Scythogondolella mosheri* (Kozur & Mostler 1976); C, STC2 (PIMUZ 40037); D, STC2 (PIMUZ 40038); E, STC3 (PIMUZ 40042). F, K, *Scythogondolella mosheri*? (Kozur & Mostler 1976); F, STC3 (PIMUZ 40043); K, STC4 (PIMUZ 40046). G, H, P, *Scythogondolella* cf. *lachrymiformis* (Orchard 2008); G, STC3 (PIMUZ 40044); H, STC1 (PIMUZ 40033); P, STC11 (PIMUZ 40086). I, *Scythogondolella* cf. *mosheri*, (Kozur & Mostler 1976); STC1 (PIMUZ 40034). L, M, N, O, *Scythogondolella lachrymiformis* (Orchard 2008); all from STC11 (PIMUZ 40082, PIMUZ 40083, PIMUZ 40084, PIMUZ 40085). Q, *Scythogondolella* sp., P_2-element; STC3 (PIMUZ 40047).

(Fig. 5B) is here documented for the first time. The latter two species do usually not appear before the *W. tardus* Zone in the late Smithian (e.g. Nakrem *et al.* 2008; Orchard 2008; Orchard & Zonneveld 2009). Therefore, this fauna might represent the transition from the middle to the late Smithian.

LMH3.- Content: *Scythogondolella lachrymiformis, Scythogondolella mosheri, Scythogondolella* ex gr. *milleri, Neospathodus* ex gr. *pakistanensis, Novispathodus* ex gr. *waageni.* Sample: STC2. Age: late Smithian.

LMH3 overlaps with the *W. tardus* Zone which indicates a late Smithian age (Dagys & Weitschat 1993). The co-occurrence of *W. tardus* with abundant, typically late Smithian conodonts such as *Sc. mosheri* and *Sc.* ex gr. *milleri* (Fig. 5C, D) underlines a late Smithian age. *Nv.* ex gr. *waageni* is a common species throughout the entire Smithian stage and was already reported previously from the *W. tardus* Zone in Svalbard (Weitschat & Lehmann 1978, Nakrem *et al.* 2008). For the first time, also *Ns.* ex gr. *pakistanensis* (Fig. 6C) and *Sc. lachrymiformis* are reported from this zone, previously only found from around the Induan–Olenekian boundary (IOB) in Svalbard (Nakrem *et al.* 2008) and the *E. romunduri* Zone in the Canadian Arctic (Orchard 2008).

LMH4.- Content: *Scythogondolella mosheri*, *Borinella* ex gr. *buurensis*, *Borinella composita*, *Borinella jakutensis*, *Novispathodus* ex gr. *abruptus*, *Novispathodus* sp. Z (Orchard 2007), *Novispathodus* ex gr. *pingdingshanensis*, *Icriospathodus zaksi*, *Novispathodus* sp. indet., *Triassospathodus symmetricus*, *Triassospathodus* aff. *symmetricus*. Sample: STC4. Age: early Spathian.

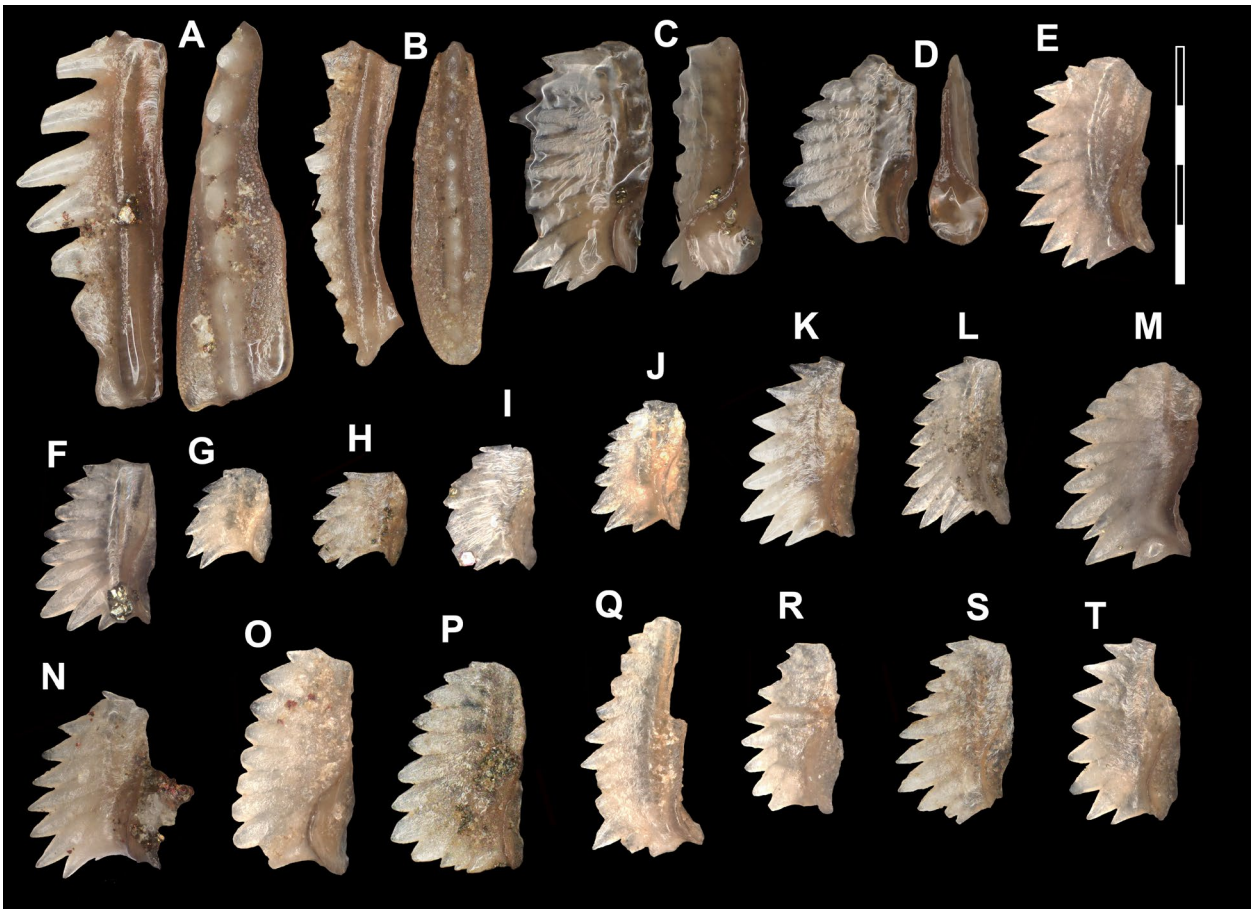

Fig. 6. digital microscope. The magnification is x80. Scale bar represents 400 µm. All specimens are P_1 elements if not otherwise specified. The orientation is standardized with the anterior side to the top, and the denticle tips to the left in 'lateral' views. Images were obtained with a Keyence VHX 6000 digital microscope. A, B, *Borinella* ex gr. *buurensis* morphotype δ (Dagis 1984); both from STC4 (PIMUZ 40048, PIMUZ 40049). C, *Neospathodus* ex gr. *pakistanensis* (Sweet 1970); STC2 (PIMUZ 40039). D, *Novispathodus* ex gr. *waageni* (Sweet 1970); STC1 (PIMUZ 40036). E, T, *Novispathodus* sp. indet.; both from STC4 (PIMUZ 40050, PIMUZ 40065). F, J, M, P, *Novispathodus* ex gr. *abruptus* (Orchard 1995); all from STC4 (PIMUZ 40051, PIMUZ 40055, PIMUZ 40058, PIMUZ 40061). G, H, I, L, *Novispathodus* ex gr. *pingdingshanensis* (Zhao & Orchard 2005); all from STC4 (PIMUZ 40052, PIMUZ 40053, PIMUZ 40054, PIMUZ 40057). K, S, *Novispathodus* ex gr. *abruptus*? (Orchard 1995); both from STC4 (PIMUZ 40056, PIMUZ 40064). N, *Novispathodus* ex gr. *pingdingshanensis*? (Zhao & Orchard 2005); STC4(PIMUZ 40059). O, R, *Icriospathodus zaksi* (Buryi 1979); both from STC4 (PIMUZ 40060, PIMUZ 40063). Q, *Triassospathodus* cf. *symmetricus* (Orchard 1995) ; STC4 (PIMUZ 40062).

For the first time, an early Spathian conodont fauna from Svalbard is here described. This LMH overlaps with the *B. euomphala* ammonoid zone which is usually devoid of conodonts in the Boreal regions (e.g. Clark & Hatleberg 1983; Hatleberg & Clark 1984; Dagis & Korchinskaya 1989; Nakrem *et al*. 2008; Orchard 2008). Most of the conodont taxa found in this LMH4 are also characteristic for the earliest Spathian UAZ8 in South China (Leu *et al*. 2022) and UAZ4 in Oman (Leu *et al*. 2023). For example, *Nv*. sp. Z (Fig. 4I) is characteristic of the earliest Spathian, as is the combination of *Nv*. ex gr. *pingdingshanensis* (Figs 4M; 6G, H, I, L) with either *Tr*. aff. *symmetricus* (Fig. 4O) or *Tr. symmetricus* (Fig. 6Q) for UAZ8 in South China (Leu *et al*. 2022). In Oman, the characteristic pair of species for UAZ4 is *Nv*. ex gr. *pingdingshanensis* and *Tr. symmetricus* (Leu *et al*. 2023). Together with the ammonoid occurrence of *B. euomphala* and the organic carbon isotope curve (around the peak of the positive excursion), it indicates that this LMH is of earliest Spathian age.

Furthermore, segminiplanate forms such as *Borinella jakutensis* (Fig. 4B), *Bo. composita* (Fig. 4D) and *Bo.* ex gr. *buurensis* Figs 4A, C; 6A, B) were recovered from this LMH. *Borinella jakutensis* was first described from the middle Smithian in Russia (Dagis 1984) but has since also been found in early Spathian strata elsewhere (Orchard 2007, Chen *et al*. 2019, Golding 2021). Similarly, *Borinella* ex gr. *buurensis* was found worldwide from around the Smithian-Spathian transition (e.g. Maekawa *et al*. 2018; Golding 2021, Orchard 2022, Leu *et al*. 2022, 2023). For *Borinella composita*, only limited biostratigraphical data are available, but a latest Smithian occurrence was already previously proposed (Dagis 1984; Orchard 2007).

Surprisingly, *Scythogondolella mosheri* (Fig. 4J) occurs within this early Spathian LMH as well. This is otherwise a well-known species from the late Smithian *Anasibirites* and *Wasatchites* beds worldwide (e.g. Orchard 2008; Nakrem *et al.* 2008; Orchard & Zonneveld 2009; Sun *et al.* 2021; Maekawa & Jenks 2021). However, given the relatively long temporal occurrence of *Scythogondolella* at boreal latitudes (e.g. Orchard 2008), surviving taxa into the earliest Spathian of this genus seems within the bounds of possibility.

LMH5.- Content: *Columbitella joanae.* Sample: STC8. Age: middle? Spathian.

With only one species identified in this horizon, an exact age determination of LMH5 is difficult. However, *Co. joanae* (Fig. 4E) has previously been recognized from the Spathian of the Toad Formation at Chowade River in British Columbia, the Sulphur Mountain Formation in the Wapiti Lake area of British Columbia, and the *Columbites* beds at Paris Canyon in Idaho (Orchard & Zonneveld 2009). Furthermore, this species was recently discovered in co-occurrence with *Tr*. ex gr. *homeri*, a typical middle to late Spathian conodont species (Golding 2021). *Co. joanae* was also recovered in the *Keyserlingites* ammonoid range from the Milne Edwardsfjellet section, 5km apart from the Stensiöfjellet section, 36m above base of the Vendomdalen Member (initially determined as *Co*.? sp. nov. K by Nakrem *et al*. (2008), afterwards re-interpreted as *Co. joanae* by Orchard (2022)). Although the thickness of the Vendomdalen Member in both sections is similar (ca. 82m at Stensiöfjellet vs. ca. 100m at Milne Edwardsfjellet), this species occurs already ca. 10m above the base of the Vendomdalen Member in our study. Moreover, *Columbitella joanae* was recently found in the slightly older *Grippia* bonebed as well (Nakrem & Orchard, 2023). Therefore, we consider LMH5 of middle Spathian age.

Palynology

Most palynomorphs recovered from the Stensiöfjellet section are poorly preserved (Fig. 7), only a few samples were moderately preserved. Generally, the palynomorph yield is very low, due to poor preservation and high abundance of other OM particles (homogenized sheets and flakes *sensu* Vigran in Mørk *et al*. 1999). Counting of palynomorphs was possible only in a few samples, and even in those the target of 250 palynomorphs could not always be reached (see supplementary data table S2: https://doi.org/10.5061/dryad.7wm37pw12). All other samples were scanned for their content. The description of the assemblages focuses first on counted samples. Further information from other samples is added. Three associations can be distinguished (Fig. 8):

Association 1.- The description of Association 1 is based on three samples from the upper part of the Lusitaniadalen Member (STA 105, STA 106, STA 106-1; 13.7–19.3 m). Assemblages are marked by the dominance of cavate trilete spores, mainly *Densoisporites* spp. Additional lycopsid spores present are *Lundbladispora* spp., *Kraeuselisporites* spp., and *Pechorosporites* spp.. However, in many instances the preservation was too poor to assign individual sporomorphs to one of these genera. Therefore, the category Kraeuseli-Lundbladi-Pechoro was created. This category includes cavate spores with morphological remnants that resemble *Kraeuselisporites, Lundbladispora*, or *Pechorosporites* but are not unequivocal. Most of them are probably corroded *Pechorosporites* species.

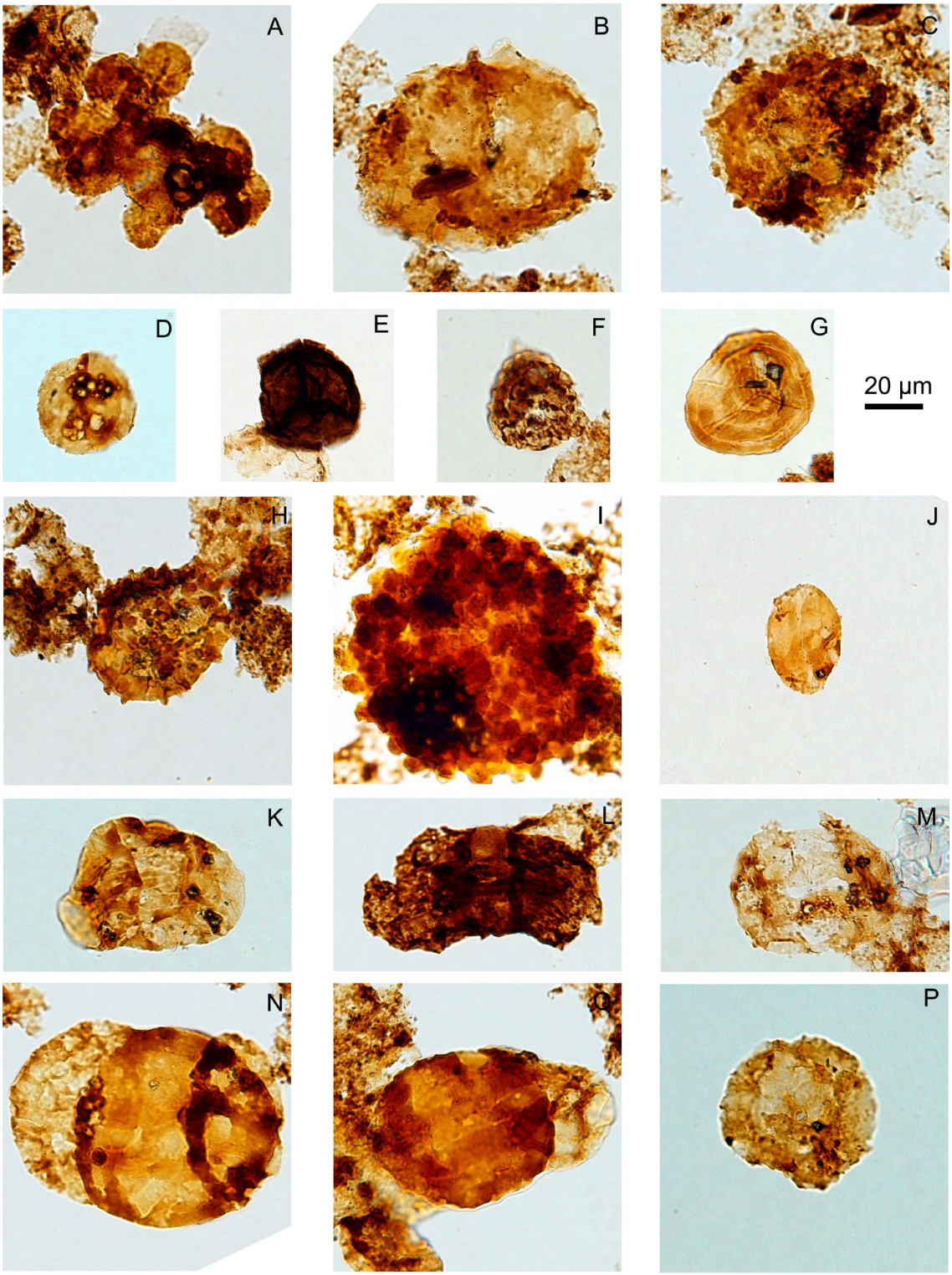

Fig. 7. Palynomorphs from the Stensiöfjellet section. Palynomorph name is followed by repository number of the slide box, slide number and Englandfinder coordinates. A, algal cyst cluster, PIMUZ A/VI 165, STA 136 a, J17/4. B, *Pechorosporites* sp. corroded, PIMUZ A/VI 165, STA 143 a, U25/3. C, *Pechorosporites disertus*, PIMUZ A/VI 164, STA112 a, M9/1. D, *Aratrisporites* sp., PIMUZ A/VI 163, STA 102 a, M6/2. E, *Densoisporites nejburgii* (dark), PIMUZ A/VI 164, STA 105 a, M26. F, *Uvaesporites sp*., PIMUZ A/VI 163, STA 103 a, W15/1. G, *Polycingulatisporites sp*., PIMUZ A/VI 166, STA 151 a, L46/1. H, *Jerseyiaspora punctispinosa*, PIMUZ A/VI 166, STA 151 a, G20/3. I, *Cyclotriletes margaritatus*, PIMUZ A/VI 165, STA 133 a, V9. J, *Cycadopites sp.*, PIMUZ A/VI 165, STA 139 a, W16/2. K, *Striatoabieites multistriatus?,* PIMUZ A/VI 165, STA 150 a, H46. L, *Lunatisporites hexagonalis*, PIMUZ A/VI 165, STA 133 a, Y35/1. M, *Lunatisporites pellucidus*, PIMUZ A/VI 165, STA 127 a, J33/1. N, *Lunatisporites noviaulensis,* PIMUZ A/VI 165, STA 131 a, N26/3. O, *Lunatisporites acutus*, PIMUZ A/VI 164, STA 124 a, Q10/2. P, *Cordaitina minor*?, PIMUZ A/VI 165, STA 146 a, W19.

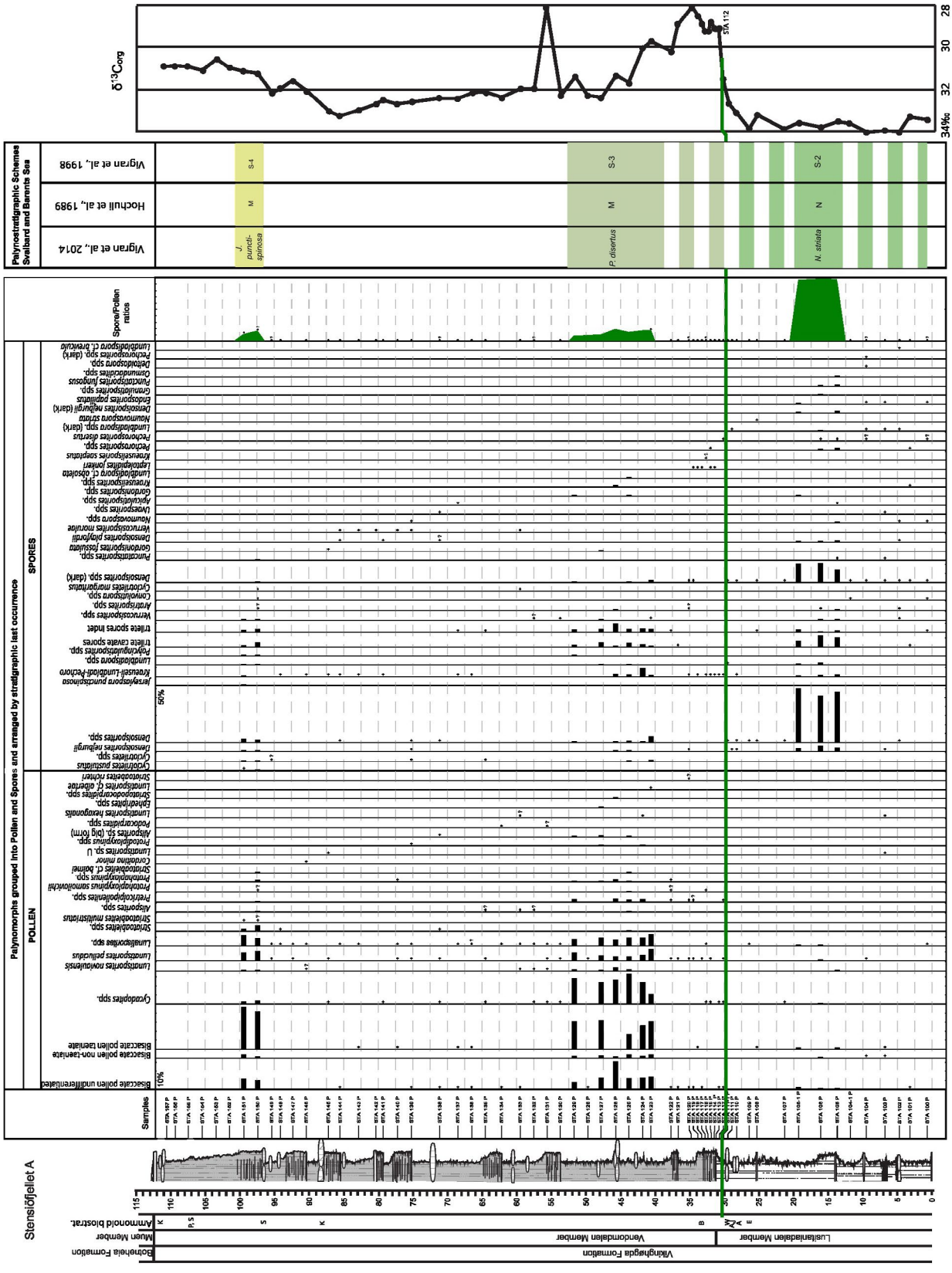

Fig. 8. Relative abundance data of spore and pollen taxa in the Stensiöfjellet succession. Palynomorph assemblages are compared with palynostratigrahical schemes by Vigran *et al.* 2014, Hochuli *et al.* 1989 and Vigran *et al.* 1998. Solid coloured intervals indicate confident identification of the palynozones (*N. striata, P. disertus, J punctispinosa*) whereas striped intervals have been tentatively assigned based on presence/absence data. Bulk organic carbon isotope data after Blattmann *et al.* (2024).

Remarkable is the bimodal preservation of palynomorphs especially apparent in *Densoisporites* spp. The main proportion of *Densoisporites* spores is light coloured (TAS 4) and corroded, while the smaller proportion is of dark brown colour (TAS 5.5) and morphologically more intact. Together, light-coloured and dark-coloured forms account for 70–80% of the total assemblage. Bisaccate pollen grains (including *Lunatisporites* spp.) are very rare, whereas 'fungal remains type 1' sensu Hochuli *et al.* (1989) are very common (Blattmann *et al.*, 2024). The dominance of *Densoisporites* spp. and the common occurrence of 'fungal remains type 1' indicate that the assemblages can be assigned to the *Naumovasporites striata* Composite Assemblage Zone (Vigran *et al.* 2014) although the eponymous species has been found only in one sample (STA 108). Assemblage N (Hochuli *et al.* 1989) and 'Svalis 2', Smithian palynozones from the Barents Sea area, have been incorporated in the *N. striata* Composite Assemblage Zone (Vigran *et al.* 2014). From the spore-pollen occurrences in the samples below and above, it can be assumed that Association 1 extends from the base of the studied succession up to and including samples STA 111-1 at 30.1m, just above the horizon with *Wasatchites* sp. and below the Lusitaniadalen-Vendomdalen boundary.

Association 2.- Association 2 comprises six samples from the lower part of the Vendomdalen Member (STA 123-STA 127, and STA 129, 40.6–51.7 m). Assemblages are marked by high relative abundance of bisaccate pollen grains such as *Lunatisporites* spp. (including *L. pellucidus* and *L. noviaulensis*) and monosulcate pollen grains *Cycadopites* spp. and *Pretricolpipollenites* spp. Spores are still present but reduced in relative abundance, also including *Pechorosporites* spp. and *Leptolepidites jonkeri*. Although *Cordaitina gunyalensis* was not found, the assemblages in the lower part of the Vendomdalen Member can be assigned to the *Pechorosporites disertus* Composite Assemblage Zone (Vigran *et al.* 2014). Based on the consistent occurrence of bisaccate pollen grains Association 2 probably extends down-section to STA 112 (30.7 m). The upper boundary could not be identified.

Association 3.- Association 3 is represented by two samples in the upper part of the Vendomdalen Member (STA 150 and STA 151, 97.4–99.4 m). The assemblages are dominated by bisaccate pollen grains, including *Lunatisporites* spp. and *Striatoabieites* spp. *Cycadopites* spp. is reduced compared to the underlying association, spores occur in low relative abundances. *Jerseyiaspora punctispinosa* is present in STA 151. The assemblages can be assigned to the *Jerseyiaspora punctispinosa* Composite Assemblage Zone (Vigran *et al.* 2014).

Discussion

The Early Triassic palaeobiogeography of conodonts

A basal Spathian conodont record from the Boreal region (Canadian Arctic, Svalbard, and northern Russia) was unknown until now (e.g. Dagis 1984; Dagis & Korchinskaja 1989; Orchard 2008; Nakrem *et al.* 2008; Nakrem & Orchard 2023). Therefore, this study gives an important insight into the paleobiogeography of conodonts during the early Spathian radiation, which just followed the late Smithian extinction event.

During the middle Smithian, the conodont fauna in Spitsbergen and in the Boreal regions in general was characterized by abundant segminiplanate elements. Although segminate forms can be found as well, the general trend is towards a less diverse segminate conodont fauna in higher latitudes. Orchard (2008) illustrated this trend by comparing conodont faunas from the Canadian Arctic, British Columbia, and the Western USA.

Orchard (2008) mentioned that compared to Smithian conodont faunas from the Arctic, those of British Columbia and the USA are equally diverse but composed differently. For example, representatives of segminate *Conservatella, Guangxidella,* and *Discretella* are rare or unknown in *E. romunduri* Zone faunas of the boreal Arctic, but are more common in contemporaneous faunas from British Columbia, and even more so in the palaeoequatorial USA, where they dominate collections from the *E. romunduri* Zone (Orchard & Zonneveld 2009; Maekawa & Jenks 2021). Similarly, segminate *P. meeki* is rare in the Arctic, more common in British Columbia, and dominant in the *E. romunduri* Zone of Hot Springs, USA. The dominant conodont group in the *E. romunduri* Zone of the Arctic is segminiplanate *Scythogondolella*, some of which are known from British Columbia but few or none of which occur in contemporaneous strata in the USA (Orchard 2007, 2008; Orchard & Zonneveld 2009; Maekawa & Jenks 2021). Amongst the segminate species, *Nv. waageni* appears to be most widespread, but is more common in British Columbia and USA successions; whereas *Ns. pakistanensis* is more common in the Arctic, and *Ns. posterolongatus* is most common in British Columbia. In Svalbard, the conodont fauna of the *E. romunduri* Zone can be best compared to the fauna of the Canadian Arctic. Where segminate forms such as *Guangxidella*, and

Neospathodus are extremely rare, species of the segminiplanate genus *Scythogondolella* are very abundant (Nakrem *et al*. 2008; Orchard 2008).

W. tardus Zone conodont faunas show much more uniformity, not only within the Boreal regions of the Canadian Arctic and Svalbard but also worldwide (e.g. Henderson *et al*. 2018; Golding 2021). The conodont fauna described from Svalbard and the Canadian Arctic is the same as that from the type locality of the *W. tardus* Zone at Toad River, British Columbia. A similar fauna occurs in the *W. tardus* Zone of the western USA, and other localities worldwide. Notably, *Sc. milleri* and *Sc. mosheri* can be found worldwide with the exception of western Tethyan Europe localities and the palaeoequatorial South China region (e.g. Shigeta *et al*. 2014; Maekawa *et al*. 2018; Maekawa & Jenks 2021; Leu *et al*. 2022, 2023). In Svalbard, the Canadian Arctic, British Columbia, and the western USA, *Sc. mosheri* is the dominant species of this zone, and *Sc. milleri* is also commonly found.

No previous studies from Boreal successions reported basal Spathian conodonts (e.g. Weitschat & Lehmann 1978; Hatleberg & Clark 1984; Dagis 1984; Dagis & Korchinskaja 1989; Nakrem *et al*. 2008; Orchard 2008; Hansen *et al*. 2018). Some alleged Spathian conodonts (Hatleberg & Clark 1984) were later re-assigned to either Smithian or late Spathian taxa (Nakrem *et al*. 2008). Surprisingly, we found a very abundant and diverse conodont fauna, which can be compared to the earliest conodont unitary association zones from South China and Oman (Leu *et al*. 2022, 2023). Notably, the recent study by Nakrem & Orchard (2023) significantly contributes to our understanding of early Spathian conodont occurrences in the Boreal realm. Their description of conodonts from the *Grippia* bonebed, dated to late early Spathian, emphasizes the prevalence of segminiplanate species, further highlighting the dominance of this conodont group in the Boreal realm during the early Spathian. The conodont assemblages documented in our study, particularly those from the middle and late Spathian, align with previous records from the Boreal realm, characterized by a sparse but segminiplanate-dominated conodont fauna (Nakrem *et al*. 2008; Orchard 2008). Similar to the Smithian, segminate forms can also be found in the middle and late Spathian in the Boreal realm but are more abundant in the more southerly basins.

Diachronous occurrence of Scythogondolella *in the Boreal realm*

It is widely accepted that the range of *Sc. milleri* is usually limited to the late Smithian *Anasibirites* beds, but especially in middle- to high-latitude areas, the range of this species can slightly expand (Orchard 2008; Orchard & Zonneveld 2009). Recently, Maekawa & Jenks (2021) discovered the occurrence of *Sc. milleri* in the latest Smithian *Condensoceras youngi* bed, and in Oman *Sc. milleri* was reported from the early Spathian (Chen *et al*. 2019). However, the validity of the latter occurrence is uncertain, primarily due to concerns arising from chemostratigraphical and biostratigraphical correlations (e.g. Maekawa & Jenks 2021; Leu *et al*. 2023).

Furthermore, in our study, we found several specimens of *Sc. mosheri* in the earliest Spathian local maximum horizon. Based on the co-occurrence of typical early Spathian species and the absence of other typical late Smithian forms, a mixing of samples can be ruled out. Also, the lithology excludes faunal mixing because of the absence of breccias or fossil condensation. The highest abundance of *Sc. mosheri* and *Sc. milleri* is in the *W. tardus* Zone. Yet the first occurrence at Stensiöfjellet of both species with a sparse abundance is already in the older *E. romunduri* Zone (Fig. 3). Other reports document a high diversity and abundance of the genus *Scythogondolella* during the middle and late Smithian in the northwestern Panthalassa region (Nakrem *et al*. 2008; Orchard 2008; Orchard & Zonneveld 2009), suggesting that this genus evolved and diversified in that region before migrating to other areas. For further remarks and taxonomic notes, see Supplementary Text S1 in https://doi.org/10.5061/dryad.7wm37pw12.

Conodont palaeoecology

According to Mørk *et al*. (1999), the Vendomdalen Member is representing a low oxygen depositional environment. It is possible that upwelling of nutrient-rich waters, in combination with acidic and oxygen-depleted seawater conditions, contributed to an increase in the occurrence of segminate conodonts. Alternatively, changes in sea level may have played a significant role. It is widely accepted that a cooling event and subsequent regression occurred during the Smithian-Spathian transition (Goudemand *et al*. 2019). Segminiplanate conodont forms, such as *Neogondolella* and *Scythogondolella*, are known to prefer deeper and cooler waters (Orchard 1996; Lai *et al*. 2001). The distribution of segminiplanate elements along latitudes appears to be a more reliable indicator of temperature compared to segminate elements (Leu *et al*. 2019).

As mentioned earlier, segminate conodonts were always present in the Boreal realm during the Smithian and Spathian substages, albeit in very low relative abundance compared to segminiplanate

forms. However, during the earliest Spathian cooling period, the relative abundance of segminate forms in Svalbard reached its peak compared to any other time within the Smithian and Spathian intervals. A recent study by Herrmann *et al.* (2015) suggests that the distribution of Pennsylvanian conodont biofacies was primarily influenced by physico-chemical properties, such as salinity, nutrients, and dissolved oxygen levels, rather than water depth, temperature, or a relatively stenohaline lifestyle (Carr *et al.* 1984; Orchard 1996; Orchard 2007; Purnell & Jones 2012; Sun *et al.* 2012; Chen *et al.* 2015). Furthermore, Jattiot *et al.* (2018) proposed a potential connection between facies and depositional environment in relation to the taxonomic composition of nektonic ammonoids. In addition to temperature, there are numerous abiotic factors that can act as stressors and thus influence both the size of conodonts and their palaeobiogeographical distribution. Nonetheless, should temperature serve as the principal determinant of conodont distribution, short warming episodes, rapid alterations in global oceanic circulation patterns, or/and sea-level fluctuations leading to deeper, enhanced thermocline might account for the observed proliferation of segminate conodonts during the early Spathian period as well.

Timing of the vegetation shift

The shift from lycophyte spore-dominated middle Smithian assemblages to gymnosperm pollen-dominated late Smithian assemblages is known from Pakistan (Nammal, Chhidru, Chitta-Landu; e.g. Hermann *et al.* 2012), the Barents Sea (Galfetti *et al.* 2007c), and North Greenland (Lindström *et al.* 2019). At Nammal (Pakistan), the uppermost sample with spore-dominated assemblages lies just below the *Wasatchites* beds. Conodont apatite oxygen isotopes indicate that a warm climate prevailed into the latest stages of the *Wasatchites* beds, and climate cooling commenced right above them, i.e. ca. 60 cm above the *Wasatchites* beds (Goudemand *et al.* 2019). From there upwards, palynological samples are bisaccate pollen-dominated (Hermann *et al.* 2012). The change from lycophyte-dominated to gymnosperm-dominated vegetation coincides with the onset of the cooling episode in the southern subtropics.

Despite the poor preservation of palynomorphs in samples from Stensiöfjellet, the position of the vegetation change can be determined based on the consistent occurrences of lycophyte spores and gymnosperm pollen, respectively. The consistent occurrence of *Densoisporites* spp. from assemblage 1 up-section includes sample STA 111-1, which is from just above the *Wasatchites* beds. Therefore, the early late Smithian *Wasatchites* beds most probably coincide with the spore-dominated interval. Additionally, the consistent occurrence of bisaccate pollen grains from STA 112 up-section, indicates that gymnosperm-dominated vegetation became established above the *Wasatchites* beds in the late late Smithian.

This indicates that the vegetation shift is probably linked to the onset of cooling and might be synchronous in southern low latitudes and northern mid-latitudes. A temperature change is indicated for the southern subtropics (Romano *et al.* 2013), whereas proxy data based on conodont apatite are inconclusive for the Stensiöfjellet succession (Luz *2022*) and are rather influenced by changes in ocean salinity.

Palynological assemblages from the Parish Bjerg, the Ugleungernes, and the Dunken formations at Hjulspordalen and Dunken in NE Greenland show a lycophyte spore dominance in the Parish Bjerg Formation and the lower part of the Ugleungernes Formation. These assemblages have been assigned to the *Naumovaspora striata* Composite Assemblage Zone, corresponding to Association 1 at Stensiöfjellet (Lindström *et al.* 2019). The assemblages reach up to a horizon containing the middle Smithian ammonoid *Arctoceras blomstrandi* at Hjulspordalen; for the Dunken succession, no ammonoid age control exists. Above the ammonoid horizon, pollen-dominated assemblages, comparable to the *Pechorosporites disertus* Composite Assemblages Zone and Association 2 at Stensiöfjellet, have been documented (Lindström *et al.* 2019). The change in palynomorph assemblages is accompanied by an abrupt positive shift in carbon isotopes. This shift, together with the presence of middle Smithian ammonoids, indicates that the late Smithian is probably completely missing in the Hjulspordalen section. Based on the assumption that *Arctoceras blomstrandi* represents the middle to late Smithian *E. romunduri* and *W. tardus* zones defined by Tozer (1994), an asynchronous vegetation shift between NE Greenland and Pakistan has been suggested (*Lindström et al.* 2019). However, *Arctoceras blomstrandi* represents the middle Smithian only, and despite questionable representatives of *Arctoceras* being found together with '*Anawasatchites*' *(=Wasatchites) tardus* in one locality on Ellesmere Island, these combined occurrences are probably caused by condensation (Tozer 1994), i.e. they do not reflect the ammonoid biostratigraphy elsewhere in the Boreal realm.

Correlation and age implications of the palynomorph assemblages

The age assignment of the *Pechorosporites disertus* Composite Assemblage Zone has previously been

based on the correlation of Svalis 3 with other records. Because of the sparse ammonoid age control, assemblages described from cores in the Svalis Dome area have been correlated with Russian palynological assemblages and with those from Svalbard (Hochuli *et al.* 1989, Vigran *et al.* 1998). The range of Assemblages M (Hochuli *et al.* 1989) includes the ranges of the *Pechorosporites disertus* Composite Assemblage Zone and the *Jerseyiaspora punctispinosa* Composite Assemblage Zone. Age control existed only for the upper part of Assemblages M (*Keyserlingites subrobustus*) (Hochuli *et al.* 1989). The presence of the ammonoid *Bajarunia* sp. in the basal part of the Vendomdalen Member shows that Association 3, and thus the *Pechorosporites disertus* Composite Assemblage Zone, are of early Spathian age.

Conclusions

This study represents a crucial advancement in unravelling the intricacies of the Smithian-Spathian transition in the Boreal realm, with a specific focus on conodonts and palynomorphs. The identification of the inaugural basal Spathian conodont fauna in the Svalbard region significantly contributes to our understanding of the early Spathian radiation, following the late Smithian extinction event. This study responds to the critical need to create a detailed mid-latitude timeline of events for the Smithian-Spathian boundary, aiming to discern whether changes during this period in low and mid-latitudes are synchronous and, subsequently, to propose potential triggers for the observed shifts.

Our examination of conodonts highlights a thriving segminate conodont population in the early Spathian *B. euomphala* Zone, challenging prevailing assumptions about their ecological preferences, especially during a phase characterized by global cooling. Concurrently, the palynomorph analysis reveals three distinct associations, offering invaluable insights into vegetation shifts and climatic changes during this pivotal period. The shift in vegetation composition from lycophyte-dominated (Association 1) to gymnosperm-dominated (Associations 2 and 3) lies right above the *Wasatchites* beds. This vegetation shift coincides with the onset of the late Smithian–early Spathian cooling event and seems to be synchronous with the vegetation shift previously recorded for the southern subtropics.

The diachronous occurrence of *Scythogondolella* across latitudes accentuates the intricate nature of conodont distribution and evolution, potentially influencing palaeobiogeographical interpretations.

To address the imperative of creating a detailed mid-latitude timeline, we underscore the necessity for a more seamless integration of conodont and palynomorph dynamics. The observed peak in segminate forms during the earliest Spathian cooling period challenges conventional interpretations and emphasizes the significance of considering both conodonts and palynomorphs to decipher the factors influencing their distribution. This integrated approach not only contributes to a more comprehensive understanding of the Smithian-Spathian transition but also aligns with the broader aim of creating a detailed mid-latitude timeline for this critical interval.

Acknowledgements.– M. Golding is thanked for insightful discussions on Olenekian conodonts and sharing data on segminiplanate conodonts in his collections. SEM imaging was performed at the Center for Microscopy and Image Analysis, University of Zurich. Nicolas Goudemand and the IGFL in Lyon are thanked for using the Keyence VHX 6000 digital microscope. This paper benefited from comments made by reviewers Charles Henderson and an anonymous reviewer. The fieldwork in Svalbard was coordinated and cooperated with the RiS ID 10772. This work is supported by the Swiss National Fonds (SNF) project 200020_160055 and CRSII5-180253.

References

Blattmann, F. R., Schneebeli-Hermann, E., Adatte, T., Bucher, H., Vérard, C., Hammer, O., Luz, Z. A. S. & Vennemann, T. W. 2024: Palaeoenvironmental Variability and Carbon Cycle Perturbations during the Smithian-Spathian (Early Triassic) in Central Spitsbergen. *Lethaia 57* (2). https://doi.org/10.18261/let.57.2.1

Blaha, U., Appel, E. & Stanjek, H. 2008: Determination of anthropogenic boundary depth in industrially polluted soil and semi-quantification of heavy metal loads using magnetic susceptibility. *Environmental Pollution 156*, 278–289. https://doi.org/10.1016/j.envpol.2008.02.013

Brayard, A., Bucher, H., Escarguel, G., Fluteau, F., Bourquin, S. & Galfetti, T. 2006: The Early Triassic ammonoid recovery: Paleoclimatic significance of diversity gradients. *Palaeogeography, Palaeoclimatology, Palaeoecology 239*, 374–395. https://doi.org/10.1016/j.palaeo.2006.02.003

Brayard, A., Escarguel, G., Bucher, H., Monnet, C., Brühwiler, T., Goudemand, N., Galfetti, T. & Guex, J. 2009: Good genes and good luck: ammonoid diversity and the end-Permian mass extinction. *Science 325*, 1118–1121. https://doi.org/10.1126/science.1174638

Brühwiler, T., Bucher, H., Brayard, A. & Goudemand, N. 2010: High-resolution biochronology and diversity dynamics of the Early Triassic ammonoid recovery: the Smithian faunas of the Northern Indian Margin. *Palaeogeography, Palaeoclimatology, Palaeoecology 297*, 491–501. https://doi.org/10.1016/j.palaeo.2010.09.001

Buryi, G.I. 1979: Lower Triassic conodonts of South Primorye. *Institut Geolojii i Geofiziki Sibirskoe Otdelenie, Akademii Nauk, SSSR, Moskva*, 1–142.

Carr, T.R., Clark, D.L. & Paull, R.K. 1984: Cordilleran Miogeocline. In: Clark, D.L. (ed.) *Conodont Biofacies and Provincialism,* 283. Geological Society of America Special Papers 196.

Chen, Y., Jiang, H., Lai, X., Yan, C., Richoz, S., Liu, X. & Wang, L. 2015: Early Triassic conodonts of Jiarong, Nanpanjiang Basin, southern Guizhou Province, South China. *Journal of Asian Earth Sciences 105*, 104–121.

Chen, Y., Richoz, S., Krystyn, L. & Zhang, Z. 2019: Quantitative stratigraphic correlation of Tethyan conodonts across the Smithian-Spathian (Early Triassic) extinction event. *Earth-Science Reviews 195* (December 2017), 37–51. https://doi.org/10.1016/j.earscirev.2019.03.004

Clark, D.L. & Hatleberg, E.W. 1983: Paleoenvironmental factors and the distribution of conodonts in the Lower Triassic of Svalbard and Nepal. *Fossils and Strata 15*, 171–175.

Dagis, A.A. 1984: Early Triassic conodonts of northern Middle Siberia. *Academy of Sciences of the USSR, Siberian Branch. Institute of Geology and Geophysics Transactions 554*, 1–69.

Dagis, A.A., Korchinskaya, M.V., Dagis, A.S. & Dubatolov, V.N. 1989: Triassic conodonts of Svalbard. In Upper Paleozoic and Triassic of Siberia *732*, 109–121). Nauka, Novosibirsk.

Dagys, A. 1999: Evolution of the family Sibiritidae and detailed biostratigraphy of the Siberian upper Olenekian (Triassic). In: Oloriz, F & Rodriguez-Tovar, F.J. (eds) *Advancing Research on Living and Fossil Cephalopods: Development and Evolution Form, Construction, and Function Taphonomy, Palaeoecology, Palaeobiogeography, Biostratigraphy, and Basin Analysis*,109–123. Springer.

Dagys, A.S. & Weitschat, W. 1993: Intraspecific variation in Boreal Triassic ammonoids. *Géobios 26*, 107–109.

Da Silva, A. & Boulvain, F. 2006: Upper Devonian carbonate platform correlations and sea level variations recorded in magnetic susceptibility. *Palaeogeography, Palaeoclimatology, Palaeoecology 240*, 373–388.

Friesenbichler, E., Hautmann, M. & Bucher, H. 2021: The main stage of recovery after the end-Permian mass extinction: Taxonomic rediversification and ecologic reorganization of marine level-bottom communities during the Middle Triassic. *PeerJ 9*, e11654, 32 pp. https://doi.org/10.7717/peerj.11654

Galfetti, T., Bucher, H., Brayard, A., Hochuli, P.A., Weissert, H., Guodon, K., Atudorei, V. & Guex, J. 2007a: Late Early Triassic climate change: Insights from carbonate carbon isotopes, sedimentary evolution and ammonoid paleobiogeography. *Palaeogeography, Palaeoclimatology, Palaeoecology 243*, 394–411. https://doi.org/10.1016/j.palaeo.2006.08.014

Galfetti, T., Bucher, H., Ovtcharova, M., Schaltegger, U., Brayard, A., Brühwiler, T., Goudemand, N., Weissert, H., Hochuli, P. A., Cordey, F. & Guodon, K. 2007b. Timing of the Early Triassic carbon cycle perturbations inferred from new U–Pb ages and ammonoid biochronozones. *Earth and Planetary Science Letters 258*, 593–604. https://doi.org/10.1016/j.epsl.2007.04.023

Galfetti, T., Hochuli, P.A., Brayard, A., Bucher, H., Weissert, H. & Vigran, J.O. 2007c: Smithian–Spathian boundary event: Evidence for global climatic change in the wake of the end-Permian biotic crisis. *Geology 35*, 291–294. https://doi.org/10.1130/G23117A.1

Golding, M.L. 2021: Abundant conodont faunas from the Olenekian (Early Triassic) of subsurface British Columbia, Canada and diversification of the Neogondolellinae around the Smithian–Spathian boundary. *Global and Planetary Change 205*, 103613. https://doi.org/10.1016/j.gloplacha.2021.103613

Goudemand, N., Romano, C., Leu, M., Bucher, H., Trotter, J.A. & Williams, I.S. 2019: Dynamic interplay between climate and marine biodiversity upheavals during the early Triassic Smithian-Spathian biotic crisis. *Earth-Science Reviews 195*, 169–178. https://doi.org/10.1016/j.earscirev.2019.01.013

Grasby, S.E., Beauchamp, B., Bond, D.P.G., Wignall, P.B. & Sanei, H. 2016: Mercury anomalies associated with three extinction events (Capitanian Crisis, Latest Permian Extinction and the Smithian/Spathian Extinction) in NW Pangea. *Geological Magazine 153*, 285–297. https://doi.org/10.1017/S0016756815000436

Guex, J. 1991. *Biochronological Correlations*. Springer-Verlag, Berlin.

Guex, J., Hungerbühler, A., O'Dogherty, L., Atudorei, V., Taylor, D.G., Bucher, H. & Bartolini, A. 2010: Spathian (Lower Triassic) ammonoids from western USA (Idaho, California, Utah and Nevada). *Mémoires de Géologie (Lausanne) 49*, 1–82.

Guex, J., Galster, F. & Hammer, Ø. 2016: *Discrete Biochronological Time Scales*. Springer International Publishing.

Hammer, Ø., Jones, M.T., Schneebeli-Hermann, E., Hansen, B.B. & Bucher, H. 2019: Are Early Triassic extinction events associated with mercury anomalies? A reassessment of the Smithian/Spathian boundary extinction. *Earth-Science Reviews 195*, 179–190. https://doi.org/10.1016/j.earscirev.2019.04.016

Hansen, B.B., Hammer, Ø. & Nakrem, H.A. 2018: Stratigraphy and age of the *Grippia* niveau bonebed, Lower Triassic Vikinghøgda formation, Spitsbergen. *Norwegian Journal of Geology 98*, 175–187.

Hansen, B.B., Bucher, H., Schneebeli-Hermann, E. & Hammer, Ø. 2021: The middle Smithian (Early Triassic) ammonoid Arctoceras blomstrandi: conch morphology and ornamentation in relation to stratigraphy. *Papers in Palaeontology 7* (3), 1435–1457. https://doi.org/10.1002/spp2.1348

Hansen, B.B., Bucher, H., Schneebeli-Hermann, E. & Hammer, Ø. 2024: Smithian and Spathian palaeontological records of the Vikinghøgda Formation in Central Spitsbergen. *Lethaia 57* (1), 1–15. https://doi.org/10.18261/let.57.1.3

Hatleberg, E.W. & Clark, D.L. 1984: Lower Triassic conodonts and biofacies interpretations: Nepal and Svalbard. *Geologica et Palaeontologica 18*, 101–125.

Hautmann, M. 2014: Diversification and diversity partitioning. *Paleobiology 40*, 162–176. https://doi.org/10.1666/13041

Henderson, C. M., Golding, M. L. & Orchard, M. J. 2018: Conodont sequence biostratigraphy of the Lower Triassic Montney Formation. *Bulletin of Canadian Petroleum Geology*, *66*, 7–22.

Hermann, E., Hochuli, P.A., Bucher, H., Brühwiler, T., Hautmann, M., Ware, D. & Roohi, G. 2011: Terrestrial ecosystems on North Gondwana following the end-Permian mass extinction. *Gondwana Research 20*, 630–637. https://doi.org/10.1016/j.gr.2011.01.008

Hermann, E., Hochuli, P. A., Bucher, H. & Roohi, G. 2012: Uppermost Permian to Middle Triassic palynology of the Salt Range and Surghar Range, Pakistan. *Review of Palaeobotany and Palynology 169*, 61–95. https://doi.org/10.1016/j.revpalbo.2011.10.004

Herrmann, A.D., Barrick, J.E. & Algeo, T.J. 2015: The relationship of conodont biofacies to spatially variable water mass properties in the Late Pennsylvanian Midcontinent Sea. *Paleoceanography 30*, 269–283.

Hochuli, P.A., Colin, J.P. & Vigran, J.O. 1989: Triassic biostratigraphy of the Barents Sea area. In Collinson, J.D. (ed.): *Correlation in Hydrocarbon Exploration*, 131–153. Graham and Trotman, London.

Hounslow, M.W., Hu, M., Mørk, A., Weitschat, W., Vigran, J.O., Karloukovski, V. & Orchard, M.J. 2008: Intercalibration of Boreal and Tethyan time scales: the magnetobiostratigraphy of the Middle Triassic and the latest Early Triassic from Spitsbergen, Arctic Norway. *Polar Research 27*, 469–490.

Jattiot, R., Brayard, A., Bucher, H., Vennin, E., Caravaca, G., Jenks, J.F., Bylund, K.G. & Escarguel, G. 2018: Palaeobiogeographical distribution of Smithian (Early Triassic) ammonoid faunas within the western USA basin and its controlling parameters. *Palaeontology 61*, 881–904.

Jeppsson, L. & Anehus, R. 1999: A new technique to separate conodont elements from heavier minerals. *Alcheringa 23*, 57–62. https://doi.org/10.1080/03115519908619339

Jeppsson, L., Anehus, R. & Fredholm, D. 1999: The optimal acetate buffered acetic acid technique for extracting phosphatic fossils. *Journal of Paleontology 73*, 964–972. https://doi.org/10.1017/S0022336000040798

Kozur, H. & Mostler, H. 1976: Neue Conodonten aus dem Jungpaläozoikum und der Trias. *Geologisch-Paläontologische Mitteilungen Innsbruck 6*, 1–33.

Lai, X., Wignall, P. & Zhang, K. 2001: Palaeoecology of the conodonts *Hindeodus* and *Clarkina* during the Permian–Triassic transitional period. *Palaeogeography, Palaeoclimatology, Palaeoecology 171*, 63–72.

Leu, M., Bucher, H. & Goudemand, N. 2019: Clade-dependent size response of conodonts to environmental changes during the late Smithian extinction. *Earth-Science Reviews 195*, 52–67. https://doi.org/10.1016/j.earscirev.2018.11.003

Leu, M., Bucher, H., Vennemann, T., Bagherpour, B., Ji, C., Brosse, M. & Goudemand, N. 2022: A Unitary Association-based conodont biozonation of the Smithian–Spathian boundary (Early Triassic) and associated biotic crisis from South China. *Swiss Journal of Palaeontology 141,* 61 pp. https://doi.org/10.1186/s13358-022-00259-x

Leu, M., Bucher, H., Baud, A., Vennemann, T., Luz, Z., Hautmann, M. & Goudemand, N. 2023: An expanded Smithian–Spathian (Lower Triassic) boundary from a reefal build-up record in Oman: implications for conodont taxonomy, high-resolution biochronology and the carbon isotope record. *Papers in Palaeontology 9*, e1481, 46 pp. https://doi.org/10.1002/spp2.1481

Lindström, S., Bjerager, M., Alsen, P., Sanei, H. & Bojesen-Koefoed, J. 2019: The Smithian–Spathian boundary in North Greenland: implications for extreme global climate changes. *Geological Magazine 157*, 1547–1567. https://doi.org/10.1017/S0016756819000669

Locatelli, L. 2023: *Inception of the Late Smithian (Early Triassic) Ammonoid Extinction: A Taxonomical Revision of the Cosmopolitan Anasibirites Fauna*. Unpublished Doctoral Dissertation, University of Zurich, 179 pp.

Luz, Z. A. S. 2022: *Characterizing Conodont Bioapatite from the Early-Triassic: An Analytical and Palaeoclimatological Approach.* Unpublished Doctoral Dissertation University of Lausanne,163 pp.

Maekawa, T. & Jenks, J.F. 2021: Smithian (Olenekian, Early Triassic) Conodonts from Ammonoid-Bearing Limestone Blocks at Crittenden Springs, Elko County, Nevada, USA. *Paleontological Research 25*, 201–245. https://doi.org/10.2517/2020PR022

Maekawa, T., Komatsu, T. & Koike, T. 2018: Early Triassic conodonts from the Tahogawa Member of the Taho Formation, Ehime Prefecture, Southwest Japan. *Paleontological Research 22*, 1–62. https://doi.org/10.2517/2018PR001

Mørk, A., Elvebakk, G., Forsberg, A.W., Hounslow, M.W., Nakrem, H.A., Vigran, J.O. & Weitschat, W. 1999: The type section of the Vikinghøgda Formation: a new Lower Triassic unit in central and eastern Svalbard. *Polar Research 18*, 51–82.

Mørk, A., Knarud, R. & Worsley, D. 1982: Depositional and diagenetic environments of the Triassic and Lower Jurassic succession of Svalbard. In Embry, A.F. & Balkwill, H.R. (eds): *Arctic Geology and Geophysics: Proceedings of the Third International Symposium on Arctic Geology*, 371–398.

Mosher, L.C. 1973: Triassic conodonts from British Columbia and the northern Arctic Islands. *Contributions to Canadian Paleontology, Geological Survey of Canada, Bulletin 222*, 141–193.

Müller, K.J. 1956: Triassic conodonts from Nevada. *Journal of Paleontology 30*, 818–830.

Nakrem, H. A. & Orchard, M. J. 2023: Conodonts from the *Grippia* niveau bonebed (Lower Triassic, Spathian), Spitsbergen, Arctic Norway. *Lethaia 56*, 1–10. https://doi.org/10.18261/let.56.4.7

Nakrem, H.A., Orchard, M.J., Weitschat, W., Hounslow, M.W., Beatty, T.W. & Mørk, A. 2008: Triassic conodonts from Svalbard and their Boreal correlations. *Polar Research 27*, 523–539. https://doi.org/10.1111/j.1751-8369.2008.00076.x

Orchard, M.J. 1995: Taxonomy and correlation of Lower Triassic (Spathian) segminate conodonts from Oman and revision of some species of *Neospathodus*. *Journal of Paleontology 69*, 110–122.

Orchard, M.J. 1996: Conodont fauna from the Permian–Triassic boundary: observations and reservations. *Permophiles 28*, 29–35.

Orchard, M.J. 2007: Conodont diversity and evolution through the latest Permian and Early Triassic upheavals. *Palaeogeography, Palaeoclimatology, Palaeoecology 252*, 93–117. https://doi.org/10.1016/j.palaeo.2006.11.037

Orchard, M.J. 2008: Lower Triassic conodonts from the Canadian Arctic, their intercalibration with ammonoid-based stages and a comparison with other North American Olenekian faunas. *Polar Research 27*, 393–412. https://doi.org/10.1111/j.1751-8369.2008.00072.x

Orchard, M.J. 2022: North American Spathian (upper Olenekian, Lower Triassic) neogondolellin conodonts. *Papers in Palaeontology 8*, e1409. https://doi.org/10.1002/spp2.1409

Orchard, M.J. & Zonneveld, J.P. 2009: The Lower Triassic Sulphur Mountain Formation in the Wapiti Lake area: lithostratigraphy, conodont biostratigraphy, and a new biozonation for the lower Olenekian (Smithian). *Canadian Journal of Earth Sciences 46*, 757–790. https://doi.org/10.1139/E09-051

Piazza, V., Hammer, Ø. & Jattiot, R. 2017: New late Smithian (Early Triassic) ammonoids from the Lusitaniadalen Member, VikinghøgdaVikinghogda Formation, Svalbard. *Norwegian Journal of Geology 97*, 105–117.

Purnell, M.A. & Jones, D. 2012: Quantitative analysis of conodont tooth wear and damage as a test of ecological and functional hypotheses. *Paleobiology 38*, 605–626. https://doi.org/10.1666/09070.1

Saito, R., Kaiho, K., Oba, M., Takahashi, S., Chen, Z.Q. & Tong, J. 2013: A terrestrial vegetation turnover in the middle of the Early Triassic. *Global and Planetary Change 105*, 152–159. https://doi.org/10.1016/j.gloplacha.2012.07.008

Scheyer, T.M., Romano, C., Jenks, J. & Bucher, H. 2014: Early Triassic Marine Biotic Recovery: The Predators' Perspective. *PLoS One 9*, e88987, 20 pp. https://doi.org/10.1371/journal.pone.0088987

Schneebeli-Hermann, E., Hochuli, P.A., Bucher, H., Goudemand, N., Brühwiler, T. & Galfetti, T. 2012: Palynology of the Lower Triassic succession of Tulong, South Tibet — evidence for early recovery of gymnosperms. *Palaeogeography, Palaeoclimatology, Palaeoecology 339–341*, 12–24. https://doi.org/10.1016/j.palaeo.2012.04.010

Shigeta, Y., Komatsu, T., Maekawa, T. & Huyen, D.T. (eds) 2014: Olenekian (Early Triassic) stratigraphy and fossil assemblages in northeastern Vietnam. *National Museum of Nature and Science Monographs 45*, 309 pp.

Stensiö, E.A. 1921: *Triassic fishes from Spitzbergen. Part I*. Adolf Holzhausen, Vienna.

Sun, Y.D., Richoz, S., Krystyn, L., Grasby, S.E., Chen, Y.L., Banerjee, D. & Joachimski, M.M. 2021: Integrated bio-chemostratigraphy of Lower and Middle Triassic marine successions at Spiti in the Indian Himalaya: Implications for the Early Triassic nutrient crisis. *Global and Planetary Change 196*, 103363. https://doi.org/10.1016/j.gloplacha.2020.103363

Sun, Y., Joachimski, M.M., Wignall, P.B., Yan, C., Chen, Y., Jiang, H., Wang, L. & Lai, X. 2012: Lethally hot temperatures during the Early Triassic greenhouse. *Science 338,* 366–370. https://doi.org/10.1126/science.1224126

Sweet, W.C. 1970: Uppermost Permian and Lower Triassic conodonts of the Salt Range and Trans-Indus Ranges, West Pakistan. In Kummel, B. & Teichert, C. (eds): *Stratigraphic Boundary Problems: Permian and Triassic of West Pakistan. University of Kansas. Deptartment of Geology, Special Publication 4*, 207–275.

Tozer, E.T. 1961: Triassic stratigraphy and faunas, Queen Elizabeth Islands, Arctic Archipelago. *Geological Survey of Canada Memoir 316*.

Tozer, E.T. 1994: Canadian Triassic Ammonoid Fauna. *Geological Survey of Canada Bulletin 467*, 1–663.

Traverse, A., 2007. *Paleopalynology*. Springer Verlag, Dordrecht.

Vigran, J.O., Mangerud, G., Mørk A., Bugge, T. & Weitschat, W. 1998: Biostratigraphy and sequence stratigraphy of the Lower and Middle Triassic deposits from the Svalis Dome, Central Barents Sea, Norway. *Palynology 22*, 89–141.

Vigran, J.O., Mangerud, G., Mørk, A., Worsley, D. & Hochuli, P.A. 2014: Palynology and Geology of the Triassic succession of Svalbard and the Barents Sea. *Geological Survey of Norway Special Publication 14*, 1–270.

Weitschat, W. & Dagys, A.S. 1989: Triassic biostratigraphy of Svalbard and a comparison with NE-Siberia. *Mitteilungen geologisch-paläontologisches Institut Universität Hamburg 68*, 179–213.

Weitschat, W. & Lehmann, U. 1978: Biostratigraphy of the uppermost part of the Smithian Stage (Lower Triassic) at the Botneheia, W-Spitsbergen. *Mitteilungen geologisch-paläontologisches Institut Universität Hamburg 48*, 85–100.

Widmann, P., Bucher, H., Leu, M., Vennemann, T., Bagherpour, B., Schneebeli-H, Ermann, E., Goudemand, N., Clare, M.A. & Burgess, S. 2020: Dynamics of the Largest Carbon Isotope Excursion During the Early Triassic Biotic Recovery. *Frontiers in Earth Sciences 8*, 1–16. https://doi.org/10.3389/feart.2020.00196

Wiman, C. 1910: Ichtyosaurier aus der Trias Spitzbergens. *Bulletin of the Geological Institution of the University of Upsala 10*, 124–148.

Zhang, L., Orchard, M. J., Brayard, A., Algeo, T.J., Zhao, L., Chen, Z.-Q. & Lyu, Z. 2019: The Smithian/Spathian boundary (late Early Triassic): a review of ammonoid, conodont, and carbon-isotopic criteria. *Earth-Science Reviews 195*, 7–36. https://doi.org/10.1016/J.EARSCIREV.2019.02.014

Zhao, L., Orchard, M.J., Tong, J., Sun, Z., Zuo, J., Zhang, S. & Yun, A. 2007: Lower Triassic conodont sequence in Chaohu, Anhui Province, China and its global correlation. *Palaeogeography, Palaeoclimatology, Palaeoecology 252*, 24–38.